POWDER DIE FILL STUDY FOR POWDER METALLURY APPLICATIONS USING NEW EXPERIMENTAL APPROACHES

By

DHANASHREE AOLE

A Thesis

Submitted to the School of Graduate Studies

In Partial Fulfillment of the Requirements

For the Degree of

Master of Applied Science

McMaster University

Master of Applied Science (2010)
(Mechanical Engineering)

McMaster University
Hamilton, Ontario

TITLE: Powder Die Fill Study for Powder Metallurgy Applications Using New Experimental Approaches

AUTHOR: Dhanashree Aole, B.E. (Metallurgical Engineering)
College of Engineering Pune, Maharashtra, India

SUPERVISOR: Dr. Mukesh K. Jain, Professor,
Department of Mechanical Engineering

NUMBER OF PAGES: CXXXIX, 139

ABSTRACT

The aim of this research is to enhance performance and durability of the final PM component by improving spatial density homogeneity at die filling stage of powder metallurgy process. In this research, powder die filling processes has been studied using a novel laboratory experimental set-up, with a ring-shaped die, for assessing die fill characteristics of thin, high precision components of interest to Gates Canada.

In this investigation, usefulness of incorporating a perforated plate at the bottom of the feed shoe to improve the density uniformity in the filling condition is assessed. With this arrangement, flow and distribution of powder during the delivery stage is monitored. The powder flow pattern observed through the transparent window is utilized for obtaining full-field displacement data using an optical measurement technique. In addition to the above, several powder flow characteristics during die filling have been studied through a series of high-speed camera recordings. The role of shoe speed, and powder properties in the development of density gradient have been experimentally assessed. A series of full-scale experiments with coloured salt as a powder medium to mimic the iron powder flow have been conducted to understand flow patterns, and segregation of powder during the filling process.

Further, a novel method of density measurement of the part in die-fill condition by heating iron powder with a polymeric resin is explored. Qualitative density data obtained from the die filling experiments, and subsequent porosity data from powder

sintering in the die have been compared, to understand the reasons for density gradient in the die-cavity.

ACKNOWLEDGEMENTS

I owe my deepest gratitude to my supervisor Dr. Mukesh Jain for mentoring me throughout this work. I am heartily thankful to Dr. Mike Bruhis for his invaluable laboratory assistance and encouragement. I am also grateful to Gates Canada Ltd. for their experimental support of the project and especially to Mr. Roger Lawcock for his encouragement and advice.

I would like to gratefully acknowledge the Mechanical Engineering technical staff members Ron Lodewyks, J.P Talon, and Jim McLaren for their patience and assistance in constructing the experimental test-rig. I am also thankful to Barry Diacon, Elizabeth Takacs, and Connie Barry for their technical assistance at various stages of this work. Many thank to my friends and colleagues for their timely help and valuable advice.

Finally, I am forever indebted to my parents and my sister for their understanding, endless patience and encouragement.

TABLE OF CONTENTS

LIST OF FIGURES

LIST OF TABLES

CHAPTER 1

INTRODUCTION

1.1. Background

Powder technology is a typical processing route of powders (metallic or nonmetallic) which provides high quality close tolerance components for different applications such as automobile, agricultural machinery, aerospace application, and pharmaceutical tablets. The process of powder metallurgy mainly consists of four stages: die filling, compaction, ejection and sintering.

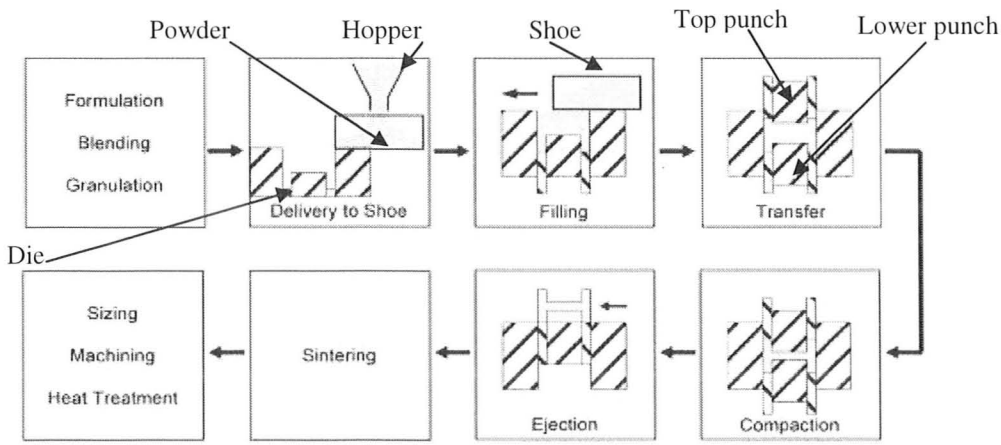

Figure 1.1. Typical powder compaction process [Sinka et al., 2007].

Fig. 1.1 shows typical powder metallurgy process which includes the preparation of the powder blend, which is then fed into the die and compacted using rigid punches.

The final part is ejected from the die-cavity and subject to post-compaction processing such as sintering, sizing, heat treatment etc. Die filling operation is the first step in P/M process in which a feed shoe connected to an overhead hopper with hoses translates over a head plate and over the die to fill the die-cavity with metal powder (Fig. 1.1). During this stage, the volume occupied by the powder in the cavity is constant and the shoe motion results in intense shear deformation, as blocks of loose powder slide over each other. The mechanical properties of powder metallurgy (PM) products are closely related to their final density, which is determined not only by the compaction and sintering process parameters but also by the filling and transfer conditions. Therefore, heterogeneity during the first step (i.e., die filling) can propagate through subsequent processes and may result in some serious defects in the final component [Wu et al., 2003a]. Thus, die filling is considered as a critical stage in the powder compaction process. From the literature review, it is noted that the compaction and sintering processes have been intensively investigated. However, investigations of the die filling field are still in their infancy.

The die filling process is governed by complex interactions of variables such as powder physical characteristics, feed rates, hopper and feed shoe design, shoe velocity, die-wall friction etc. Hopper and shoe are the two most critical components of the powder delivery system. A nonuniform powder delivery from the hopper to the feed shoe results in variation in the head pressure, and together with the flow rate and other flow characteristics translates into variation in component spatial density and dimensions. Moreover, the shoe capacity, shape and velocity, amongst other factors, determine the distribution of the powder in the die. The friction between the shoe wall and powder

restricts the movement of the powder, and thus, contribute to the variation in the spatial density of the part. The major concern is the uneven filling of powder in die-cavity. The nonuniform density in different locations of the component in the initial stage of powder metallurgy process leads to internal cracking during compaction or warpage during sintering [Kim, 2007].

A comprehensive understanding of powder flow from the feed shoe to the die-cavity is lacking. Therefore, there is a further need to review the die fill system independently to explore the various parameters that affect the density distribution of the powder in the die-cavity. Improvements to the current delivery systems have the potential to provide a cost-effective solution for manufacturing the defect-free high-precision PM parts. In recent work, a novel die-fill test rig with a transparent die and the shoe was considered to observe the flow characteristics of the powder under various conditions.

Wu and coworkers were the first to explain with the experimental studies of the die filling that net filling rate of powder in the die-cavity is improved with vacuum filling. The interaction between the powder flow and simultaneous flow of air in the opposite direction affects the final packing of the particle in the die. They also reported that as the shoe velocity increases filling rate drops, due to incomplete filling [Wu et al., 2003a]. Later studies were motivated by this work and filling in the air, and vacuum was investigated in further detail [Sinka et al., 2009]. A convenient technique of X-ray computerized tomography was also suggested by many researchers to get the detailed information on the bulk density distribution throughout the compact. However, the density distribution in a compacted sample did not explain the initial factors which have

actually affected the density homogeneity. Recently, Burch et al., (2008) investigated the initial density distribution after filling by sintering the loose powder and by examining the die in filled condition with X-ray tomography technique. However, moving the whole die in the filled condition for testing and sintering the powder is not very convenient procedure to get the accurate density distribution data. Thus, it is important to establish a reliable method for measuring the density distribution in die-fill condition for any die geometry without affecting its particle filled condition.

1.2. General objective

The first general objective of the proposed work is to improve the fundamental understanding of the die filling process. The work also focuses on quantifying the main factors that influence initial density distribution of the powder in the die. This objective is addressed; by observing the motion of the particles in the shoe with varying shoe velocity and other characteristics, and by monitoring the flow of powder in the die through the perforated plates placed at the bottom of the feed shoe of different patterns. The powder segregation from a moving shoe into the die, and particle displacements in the die-cavity during the filling process for a range of experimental test conditions are also tracked using high-speed, high-resolution camera and a displacement analysis system.

The second general idea is to measure the density distribution of the powder body in the die prior to compaction. For ex-situ density distribution measurements, the powder has to be bound together without applying pressure. Therefore, experiments are carried out with thermoplastic resin binder followed by cutting sections of interest, and then performing quantitative porosity and density analysis. The goal here is to develop a

quantitative experimental frame work to understand the density distribution in different positions within the die as a function of process parameters. This thesis describes the development of a feeding mechanism using a thick perforated plate at the bottom of the shoe for controlling the powder flow, and further enhances the distribution of powder in the die-cavity. This thesis also summarizes the impact of powder characteristics on the powder flow type and density uniformity in the die-fill condition.

1.2.1. Specific objectives

1. To study the effects of powder flow behaviour during die filling and segregation at different stages of the filling by using a high-speed and high-resolution optical imaging system.
2. To correlate the effect of shoe velocity on initial density distribution in the die-cavity.
3. To critically examine the use of perforated plate (or filters) at the bottom of the shoe, and the effect of different pattern of holes on the flow rate and distribution of powder in the die-cavity.
4. To assess the quality of surface images taken from the transparent wall-section of the die towards surface porosity determination by using image analysis software.
5. To correlate surface porosity measurement data obtained from image analysis software with the displacement field data obtained from Digital Image Correlation (ARAMIS) software.

6. To develop a technique for binding the loose iron powder in the die-fill condition, by using a thermoplastic resin.
7. To utilize a resin-bonded iron powder sample from the filled die in conjunction with gamma ray densitometry for obtaining bulk density data.

CHAPTER 2

LITERATURE REVIEW

In this section, a brief literature review in three critical areas associated with the die filling process is presented.

2.1. Powder handling and delivery

Powder delivery system includes hopper, a feed shoe which moves linearly back and forth over a die opening, and a flexible hose connecting both of these components. Many researchers have noted a correlation between powder flow and powder properties. The powder properties such as particle size, size distribution, shape, bulk density and surface properties influence the flow behavior of the powder from hopper to the feed shoe and finally to the die-cavity [Prescott et al., 2000]. During the flow in the delivery system, the particles may dilate, contract or flow at a constant volume under the influence of friction from the path of travel or the shear stress due to motions of the shoe. The flow property of the powder is typically described in terms of the angle of repose which forms between the free surface of the powder and the horizontal base when the powder stored in a funnel is dropped from a specified height. Typically, the powder with superior flow rate makes a low angle of repose. The flow properties have been also related to the cohesion and internal friction between the particles [Prescott et al., 2000].

Some studies report beneficial effects of pre-treatment or conditioning of powder particles before feeding in the hopper [Reg et al., 2008]. The conditioning involves gentle displacement of the whole powder sample, loosening and slightly aerating it into a homogenized and reproducible state to avoid caking and agglomeration in the powder bed. With the addition of lubricants, friction between the particles reduces, increasing the flow rate of the powder. However, excessive addition of lubricants in the powder can decrease the flow rate. Studies into the application of thin resin coating on the particles has been undertaken to make the particles spherical, and reduce the friction between them. During the sintering process, the resin vaporizes at the high temperature and bonds the particle strongly. In applying such coatings it is essential to minimize the amount of lubricants in order to minimize part shrinkage and porosity.

In addition, the operating conditions such as moisture, aeration, temperature, and static charge affect the flow rate. More recently, Zahrah and coworkers proposed a method of reducing the inter-particle friction during powder transfer using a fluidized shoe [Zahrah et al., 1999]. The bed is loosened, by flowing gas over the solid particle from bottom to top, to facilitate the movement of the particles facilitate.

Powder can flow through a hopper giving to main flow regimes namely mass flow and funnel flow. In mass flow, which is desirable in a hopper, all powder in the hopper is in motion. Prescott et al., (2002) explained that the mass flow from a hopper reduces the extent to which the segregation affects the powder. They also demonstrated the funnel flow of powder which forms active flow region above the outlet and non-flowing powder at the periphery. The funnel flow regime is also called as first-in-last-out flow since

material that has entered the hopper first and resides at the sides of the hopper will remain there until all other material above it has collapsed from the walls above. In a rathole regime, the material along the edges of the bin remains in place and doesn't exit the container. A very common problem with the powder flow through a hopper is arching where the powder mass gets stagnant and doesn't flow through the hopper outlet (Fig. 2.1).

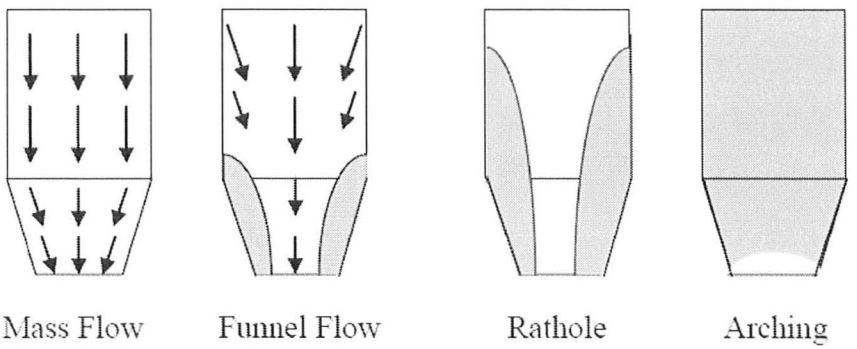

Figure 2.1. Powder flow regimes from a hopper [Emery, 2008].

The adaption of aeration and fluidization improves the powder flow-ability and works well for the powder with poor flow-ability [Prescott et al., 2000]. The major problems with the current delivery systems include transportation of the powder mass to the overhead hopper, its transfer through the flexible hose to the shoe, horizontal transport, and excessive contact with unintended surfaces. The material has to travel a long route before filling the die-cavity. This can result in an increase in the moisture content, cohesion, and also the contamination of the powder source. Another foremost concern is the powder bridge formation in the hopper, shoe, and the die. As depicted in Fig. 2.2,

mass flow works well as long as the flow of the powder is vertical [Johnson et al., 2006]. Polished finishes in the hopper internal surface, steep angle, vibration, compressed air, and rakes all have been used to modify the flow from the hopper. The bridge configuration creates nonuniform distribution of powder in the die that remains throughout the compaction stage, and ejection sequence.

During the flow of a granular mixture, spherical particles may settle more rapidly because of their smaller surface area (than say an irregularly shaped particle) causing less frictional drag force assuming that all other factors (size, mass etc.) are the same. The size distribution in a powder blend has to be considered because large particles having more mass than the small particles (assuming that their density is uniform) will settle down faster due to greater effect of gravity on them.

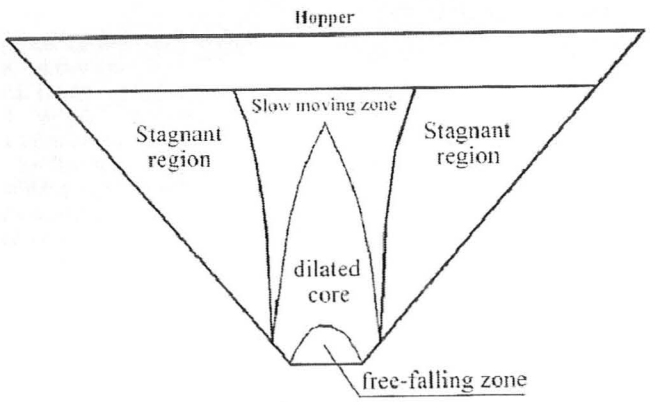

Figure 2.2. Flow regions for powder discharging from a wedge-shaped hopper [Wu et al., 2003b].

Many papers have demonstrated the problems faced in the bulk handling and inhomogeneous mix at the point of delivery. New designs using compressed air have

been considered useful in the recent years. Amongst these, the work of Johnson and coworkers, utilizes powder transfer using vacuum in conjunction with a rotary valve and a directional nozzle over the die cavity. They were successful in eliminating the overhead bulk handling and in increasing the homogeneity of the mix [Johnson et al., 2002]. The achievement was in minimizing the transfer of the powder to the point of use on the floor level to avoid the entrapment of air in the die-cavity. The device consisted of a tubular rotary powder feeder that resulted in an increase in the powder mass, and slope beyond the angle of repose. Also, included in the design was a cone shaped component at the exit that reduced the powder flow, and allowed the powder mass to lock when rotation stopped, making appropriate use of friction and gravity. A sensor was mounted in the directing nozzle that sends signals about the shoe position and powder fill condition (Fig. 2.3). The uniqueness of the design was that the falling sections rolled over each other, redistributing the particles in the powder mass. The studies of Johnson et al. highlight the role of design of the feed shoe and importance of changing the location of the powder feeder in increasing the homogeneity of the powder blend and in reducing the effect of friction between shoe wall and particles to improve the powder flow to the die-cavity.

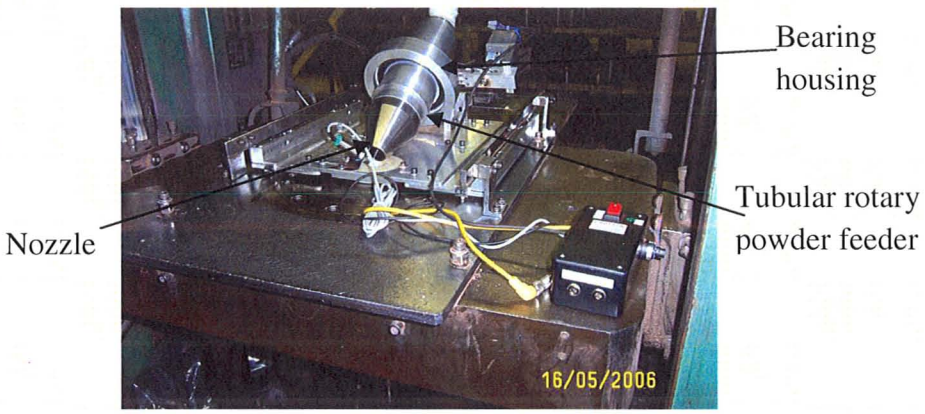

Figure 2.3. Rotary feeder device design [Johnson et al., 2002].

2.2. Powder flow into a die

The parameters which affect the flow of powder into a die can be divided into three main categories: Powder characteristics, design of the die filling equipments, and operating conditions. Powder characteristics include particle morphology, bulk density of powder, cohesive index, surface properties, and angle of repose. The die filling equipment design includes shoe and die geometry and the operating conditions comprise of shoe velocity, vibration of the die or shoe, use of compressed air, presence of moisture in the powder and number of shoe passes. There are two main die-filling techniques, the commonly used gravity filling, and suction filling. In gravity filling, the powder drops under its own weight as the shoe moves over the die-cavity. Pressure difference generated during the filling process plays an important role in determining the efficiency of the die filling process. As the powder flows into the die, the pressure builds up opposing further

accumulation of the powder. However, suction filling creates negative pressure difference as the lower punch moves down, which carries interstitial air in the pore along with the particles in the die-cavity [Motazedian et al., 2007].

Wu et al. [2003a] indicated that rate of filling decreases as the particle irregularity increases and as the average particle size decreases. High filling density is desirable for die filling, and the following, compaction process. Recently, multi-station filling presses have been introduced to speed up the production of PM components. It is extremely important in such cases that the deposition of powder is uniform in multiple dies. Therefore, some initiatives need to be taken on this front, to rectify the problems arising due to nonuniform filling.

In recent years, the effect of shoe kinematics on powder flow into a die has been investigated. Wu et al., (2003a) introduced the concept of a critical velocity, the maximum shoe velocity at which a standard die fills completely as a measure of flow-ability. At higher shoe velocities, the powder moves towards the back of the shoe due to inertia when the shoe accelerates from rest. This results in a nose-shaped pattern in the powder mass which develops a large gap between the front wall of the shoe and powder mass in the die. Furthermore, this leads to densification of the powder in the shoe due to collapse of the voids under intense motion. The cohesion of the particles increases which may decrease the flow-ability of the powder in the die. Bulk flow in the cavity prevails when the shoe moves quickly to inefficient filling [Wu et al., 2003a and b].

Furthermore, Kim proposed a fascinating approach dealing with the use of filters at the bottom of the feed shoe to increase uniformity of the die fill. When a filter is

incorporated at the bottom of the shoe, it breaks the bulk powder flow into a free vertically downward flow [Kim, 2007]. Two types of filters with different arrays of holes (linear and staggered) in a plate, as well as different volume of the feed shoe versus the volume of the holes in the filter, were considered. A lower volume of holes in the filter has the effect of confining the movement of the powder particles between the shoe and the die (below the filter), thus helping with the downward movement of the powder. The staggered array of holes in the filter shows a secondary movement of the particles, when they pass over the highest point of the filter, and the shoe changes its direction from forward to backward. The authors also described the importance of shoe design, and specifically, the number of shakes of the shoe when it moves to the top of the die opening. Shaking, typically 2 or 3 times, also helps improve the density distribution but leads to some reduction in part production rate. There is limited quantitative understanding of the use of filters, and shakes for achieving fill density uniformity [Kim, 2007].

2.2.1. Types of flow in the die-cavity

Cocks and coworkers stated that during gravity die filling when shoe moves over the die-cavity, different types of flow occur. Nose flow occurs when the top surface particles cascade into the die creating a nose-shaped profile by the initial acceleration of the shoe. They discovered that small amount of powder in the shoe, low shoe velocity, and large die opening promotes nose flow. Wu et al., (2003a) found that nose flow promotes faster evacuation of air and thus, high powder flow rate can be achieved. As the shoe moves further over the die-cavity, particles from the bottom layer of the shoe starts

filling the die, which is known as bulk flow of powder (Fig. 2.4). Bulk flow dominates when the shoe moves with high velocity. In this work, intermittent flow is also mentioned which takes place when a powder with poor flow-ability is used. In such cases, agglomerates of particles are detached from the bottom of the powder mass in a very irregular manner [Wu et al., 2003a and b]. The vertical flow of flow of powder from a filter, as studied by Kim, breaks the bulk of the powder mass and powder flows freely through the holes in the die.

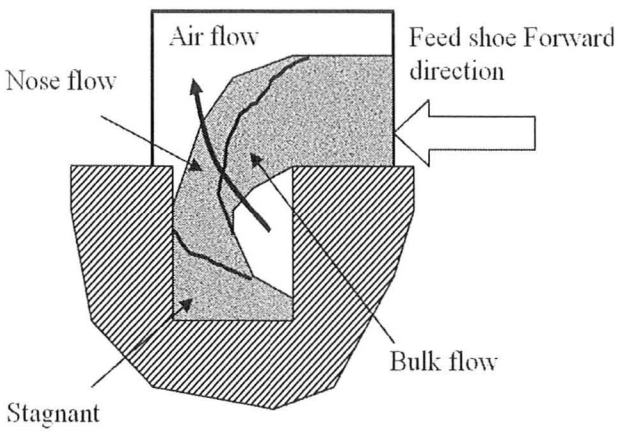

Figure 2.4. Typical die filling process [Wu et al., 2003a].

2.2.2. Influence of Shoe Kinematics

The feed shoe velocity has a significant impact on the powder flow and its segregation during the die filling process, and consequently it also affects the distribution and packing of the powder particles in the die-cavity. At lower shoe velocity, the tip of the nose (front stream of the powder) translates slowly over the die-cavity; therefore, deposits more powder in the die. However, at higher shoe velocity, powder is delivered

by the bulk flow from the bottom of the shoe. It is obvious that the top surface particles travel with high-velocity at high shoe velocity, and more particles flow into the die. There exists a critical shoe velocity at which the filling rate is the maximum, further as the shoe velocity increases filling rate decreases. In addition, bulk flow can cause interlocking effect in the powder which may results in inefficient filling; therefore, at higher shoe velocity low fill-ratio is obtained [Wu et al., 2003a]. Hjortsberg et al., (2002) investigated the effect of shoe velocity on density variations in a ring-shaped die-cavity. They found that during die filling, the kinetic energy of moving particles can be partially transferred into the die cavity, where it causes rearrangement of the particles and compaction. The increase of shoe speed results in an increase of kinetic energy of particles and hence in an increased densification in the die.

Another feature of the shoe kinematics is the shaking of the shoe filled with powder. It is found that shaking (or vibrating) the shoe above the die during the filling also helps in breaking up the cohesion and the arching of the particles [Faikin et al., 1976].

2.2.3. Effect of air flow

The air originally present in the die must be evacuated as the air entrapment results in void defect in the final part. The powder flow can get much disturbed due to the powder and air flow interaction inside the die. The influence of air was evaluated by Wu and Cocks by conducting die filling test in the air and vacuum. They found that powders flow freely and rapidly in a vacuum, except for some highly cohesive powders. In this

study, they also revealed that, in the absence of pressure difference, the flow behavior in suction filling is similar to that in gravity filling [Wu et al., 2003b].

The presence of air leads to a negative pressure gradient which can prevent the powder from flowing into the die and slow down the filling process. Wu et al. demonstrated that, for geometries of the high-aspect ratio, there is an increased risk of air entrapment and bridging of the powder. This is more likely to occur for powder with irregular particle shapes than for uniform shape particles. The small and low density particles are sensitive to the air and therefore, the flow rate of small particles is more uniform in vacuum [Wu et al., 2004].

It is evident that the shoe kinematics also affects the evacuation of the air out of the die. At high shoe velocity, due to less filling time, air gets entrapped in the powder. This builds up pressure in the die which prevents further flow of powder into the die. As a result, density distribution inside the die can become uneven. The die-filling process with the aeration method has been explained by Reg et al., (2006). He indicated that a powder which aerates enough to flow easily and degenerates sufficiently quickly ensures complete die filling. He also confirms through his experiments that the powder which instantly releases entrained air, allows more complete filling of the die. Further, Prescott et al., (2000) mentioned that permeability of a powder (its ability to allow air to pass through it) controls the discharge rate and it can also be used to calculate the settling time required for the fine particles.

Faikin et al., (1976) found that decreasing intensity of the filling not only increases the density in the poured condition of the part, but also decreases the time required to pack them in the die-cavity. The intensity of filling was varied by changing the discharge orifice diameters of the hoppers. They quoted that the best method to regulate the intensity of pouring is to change the transverse dimensions of the discharge orifice of the hopper. Further, a vibrating-die system was employed to shake the die during filling, so that the particles rearrange themselves faster and more mass of powder is filled in the cavity. They found that in a vibrating die the optimum intensity of pouring depends on particle diameter, cross-sectional area of the part being shaped, density of the powder material, relative density of the part after shaping, time for one vibration period, and frequency of vibration. The intensity of pouring was calculated in g/sec which is similar to the filling rate of powder during filling. They concluded that the intensity of powder deposition into the die can be increased on an average five times, at the same density of parts, by applying the vibrating die system. Also, there exists an optimum intensity of pouring to get maximum density in the die-fill condition with least packing defects such as bridges and arches in the poured powder [Faikin et al., 1976].

2.2.4. Influence of powder level in the shoe

The powder level in the shoe affects the filling rate. Maintenance of a horizontal powder level within the fill shoe as the powder is being discharged results in uniform head pressure during die filling. Sawayama and Seki (1999) found that if the powder bed is low in the shoe then the top layer powder flows rapidly into the die-cavity, creating a nose shaped profile and higher filling rate is obtained. A low net filling rate is obtained if

the powder level in the shoe is very low [Schneider et al., 2005]. Schneider et al. explained that when the bulk flow dominates at higher shoe velocity, filling rate is dependent on a critical level of powder in the shoe, above which the filling rate is independent of the height of powder bed in the shoe. A cohesive powder requires a greater critical powder level in the shoe than a smooth easy flowing powder. If the shoe is fully filled with powder then nose flow will not occur and consequently, only bulk flow will contribute in filling. The powder level in the shoe also affects the gap or depression created in front of the shoe during the initial acceleration of the shoe.

In gravity filling, as the powder level drops in the hopper placed over the shoe then amount of powder discharged into the die varies and part consistency is lost. A uniform level of powder in the fill shoe is necessary to maintain equal head pressure from the powder mass. Initial density variation inside the die-cavity is less, if the head pressure is uniform [Johnson et al., 2002].

2.2.6. Influence of Die Geometry

Die geometry influence the flow rate and flow pattern during die filling. The powder flow behavior in simple and complex die-cavities was investigated by Wu et al., (2003c). They found that the kinematics of flow becomes complex in a stepped die. In this complex shape die, the top region was a wide cavity and the bottom region formed a narrow section. During the powder delivery, the powder fills fastest at the center of the die, making a powder heap on the step. As this powder heap spreads across, the air in the narrow opening gets trapped and pressure rapidly builds up. The air trapped escapes from the thinnest section of the heap at an angle of 45^{o}, and more powder deposits in the top of

the outward flowing air and significant turbulence is created in the incoming stream of powder [Wu et al., 2003b]. Further, Bruch et al. explained that for simple shapes (cylindrical shape) there is little variation in the final density distribution even for different vertical (top and bottom) fill-density distributions with the same mass of powder. However, for complex die geometries, final density range is a lot higher due to nonuniform fill density distribution [Burch et al., 2008]. For a ring-shaped die-cavity, Hjortsberg et al., (2002) found that the fill-density in the sections parallel to the shoe motion is higher than in the other regions.

2.3. Segregation during powder flow

Different segregation mechanisms were initially identified by Silva et al. (2000) namely trajectory, air flow, rolling, angle of repose, embedding, impact, push away, displacement, percolation, fluidization, agglomeration, and concentration drive displacement. Segregation pattern during the powder flow can influence the final particle packing in the die. This is a typical problem with every powder flow which ultimately affects the fill density. When a mixture of different size particles flows, fine particles percolate down through the powder matrix and deposit at the bottom, whereas large particles remain at the top of the die. The fact is larger particles have small angle of repose than the fine particles; thus, larger particles flow over smaller particles with high speed and segregate nonuniformly. The powder flow from a shoe interacts with air during filling, the drag force of air lifts up the light particles leading to the segregation of the powder mass. In addition, the small and angular particles flow with low velocity due

to stronger frictional force during filling. Therefore, different trajectories of powder flow are observed depending on particle size and shape.

It was found that by using a vibrating die radial segregation can be reduced, because of inner mass of fines get leveled off (Lawrence and Beddow, 1968). The vertical segregation was found to be dependent on the frequency and amplitude of vibration.

2.3.1. Avalanche Behavior of powder

Avalanche is a rapid flow of powder substance down a slope. The avalanche occurs when the balance between cohesion of particles and gravity breaks. The flow of powder depends on the powder characteristics such as static charge, particle size, morphology, surface area, and absolute density. The purpose of studying avalanche is to characterize the fluidity and cohesion of the powders, which affect the final distribution of particles in the die during the filling process [Lavoie et al., 2002].

Koeppe et al. (1995) explained that the segregation occurs in each avalanche where the segregation pattern crucially depends on the size and shape of the powder .When a granular mixture differing in size and shape flows, the large particles with lower density or round shape are being found closer to the top of the flowing layer. This leads to longer travel time of the particles before they come to rest, but small particles cannot roll easily over the large particle surface. In such cases, the larger particles are found at the bottom of the pile, whereas the smaller particles remain at the top. Lavoie et al., (2002) has described three stages of avalanche namely pre-avalanche stage, avalanche, and post-avalanche. Pre-avalanche is a stage where cohesion forces maintain the particle

arrangement stability. These cohesion forces are divided into two categories; extrinsic and intrinsic cohesion. In extrinsic forces, particles are bound together due to environmental factors, whereas in intrinsic cohesion the particles remain bonded with the internal force, depending on the nature of the particles. At the time of the avalanche, two phenomenon take place; the distance covered by the particles and the segregation of the surface. The avalanche created is sensitive to the properties of the powder and the kinematics of the shoe motion. The changed slope of powder following the avalanche can be seen in the post-avalanche state.

Lavoie and coworkers investigated in detail the avalanche behavior of different powder at various speed with the Aeroflow instrument (a specialized instrument). They established two new quantitative indices characterizing the cohesion, and fluidity of the powders. The cohesive index indicates the capacity of the powder to be agglomerated. It also explains the particles arrangement stability and expresses the vector of the internal force which can help in the selection of the mixing operations. The investigation of the avalanche behavior in a die-filling process can be done by studying the behavior of powder under dynamic condition [Lavoie et al., 2002].

2.4. Density Measurement Techniques

Puri and Dhanoa, (1998) developed a real-time cumulative mass deposition tester, which is a convenient and effective tool to measure the uniformity of powder distribution in the complex dies. These researchers have used this tester to estimate the uniformity of the deposition of different powders in the die. Die fill density distribution has been measured using X-ray computerized tomography (or CT scan) [Xie et al., 2006]. Its

major strength for die fill studies is that it can provide useful powder bulk density distribution in the dies. However, it cannot record real-time bulk density distribution for the entire filling process. Another limitation is that it is often not practical to transfer a filled die with loose powder to the CT scan machine without displacing the powder. Further, the CT scan equipment is expensive especially if used in-situ. It is not readily available even for research use and certainly not very practical for industrial use. The use of tactile sensors was explored as a novel means of assessing density uniformity of powders in molding dies prior to compaction by Demetry et al., 1998. Nonuniform mass distribution after the die filling process was detected as gradients in the transmitted pressure by a tactile sensor located at the bottom of the die. An interesting method of powder sintering of iron powder was performed to determine the density of the loose powder in the filled die by Burch and coworkers. The powder was heated to 900^{o}C for 2 hrs and then cut to observe the distribution of particles in different sections under an optical microscope [Burch et al., 2008]. As an alternative to metallographic techniques, CT scan can also be utilized ex-situ once a method for binding the powder can be developed. The use of thermoplastic resin in particulate form to bind the powder after filling in the die might help to quantify the density measurement of loose particles in the filled condition. However, current literature suggests that no such attempts have been made. A method of binding powder particles using thermosetting resins was investigated to get powder parts without changing the original properties of the powder material. The resin acts as a binder under low temperature curing and the binder removal can be accomplished by thermal means without a separate de-binding step [Brasel et al., 1991].

This rather promising method is yet to be applied to die-fill studies to measure the density distribution of the powder in the die-cavity.

Other radiation methods for density analysis include fast neutron scattering and attenuation technique as well as gamma ray densitometry. Georg explained that gamma densitometer is fast and accurate method of measuring the void fraction in green and sintered compact. The main advantage of gamma ray densitometry is that no special preparation of sample is required, and sectional densities can be determined without cutting the part [Georg, 2001].

2.5. Summary

There is very little information available in the literature on the effect of segregation of powder on flow patterns and particle packing in the die during the die filling process. The coloured powder bed numerical models were considered few times to investigate the segregation behavior of a mixture of powder in a die filling process under different conditions. However, the data from the numerical study sometimes overestimate the real experimental parameters. In this study, coloured salt was used as a powder medium to understand the flow behavior of powder from a moving shoe on a macroscopic scale. A critical study on the powder flow pattern and final particle packing inside the die-cavity was performed and also compared with the actual metal powder flow (iron powder) by recording the complete die filling process.

A perforated plate insert at the bottom of the shoe to change the flow pattern of the powder during filling was a promising approach undertaken by Kim, but a detailed

investigation on the perforated plate pattern and its effect on the uniformity of powder flow in the die-cavity is still lacking. Therefore, two new designs of perforated plates were proposed in this study to control the flow of the powder into a ring-shaped die and to understand the change in the segregation behavior of the powder, which in turn will affect the powder distribution in the die-fill condition.

The high speed video systems were used before by many researchers to observe the flow of the powder during filling in different die geometries under various conditions. Also the strain measuring methods were applied to the compacted sample to study the particle deformation in different locations at different pressures. However, the measurement of segregation in terms of displacement of particles during filling to study the reason for the non-uniform powder distribution in the die has been investigated for the first time in this research. The displacement of the particles in top and bottom regions of the die-cavity during different stages of filling is tracked by using Digital Image Correlation (DIC) method.

In the die filling study, the main challenge is to obtain even density distribution in the part after filling so that a defect free compact can be produced. For this reason obtaining accurate quantitative data on the initial density distribution in the die-cavity prior to compaction is crucial so that the usefulness of the modified experimental parameters can be justified. Thus, in this research a method of binding the powder particles in the filled condition by using a polymeric resin was studied, so that the resin-bonded (solid) part can be taken to gamma ray densitometry to measure the void fraction

at different locations. This technique has been developed in order to overcome many of the drawbacks of the previous performed density distribution measurements.

CHAPTER 3

METHODOLOGY

In this chapter, the experimental methodology used for die filling and density measurement techniques are described. Also described are the physical properties of two types of powders (metallic and non-metallic) used in this study.

3.1. Raw Materials

Two different powders; namely, ATOMET 1001 water atomized raw iron powder and salt powder were used to understand their flow behavior during the filling process. General characteristic of the powder materials are shown in Table 3.1. The iron powder was procured and supplied by Stackpole Inc. (now a part of Gates Canada Ltd). The powder morphology was evaluated by image analysis, and other properties such as bulk density and angle of repose were measured with weighing pan and digital camera images respectively. Both iron powder and salt powder comprised of irregular shaped particles (Fig. 3.1a and b). The methods for calculating the powder properties are described in Section 3.7.

A mixture of raw iron and polyethylene powders was used for the ex-situ powder heating experiments to explore the density distribution of iron powder in die-fill condition. Fine polyethylene powder had a particle size of 100-750 μm and a bulk density of 0.24 g/cm^3.

Table 3.1. Composition and general properties of powders used in the die filling tests.

ATOMET 1001 Iron Powder	
Composition (wt %): Fe- 99.4 , C- 0.2, Mn-0.003	
Apparent Density (g/cm^3)	2.95
Flow-ability (g/s)	26
Angle of repose	20- 23^o
Particle Size (micron)	wt%
+250	10
-250/+150	65
-150/+45	25

Salt Powder	
Composition (100%): NaCl	
Apparent Density (g/cm^3)	0.294
Flow-ability (g/s)	40
Angle of repose	26-29^o
Particle Size (micron)	158-748

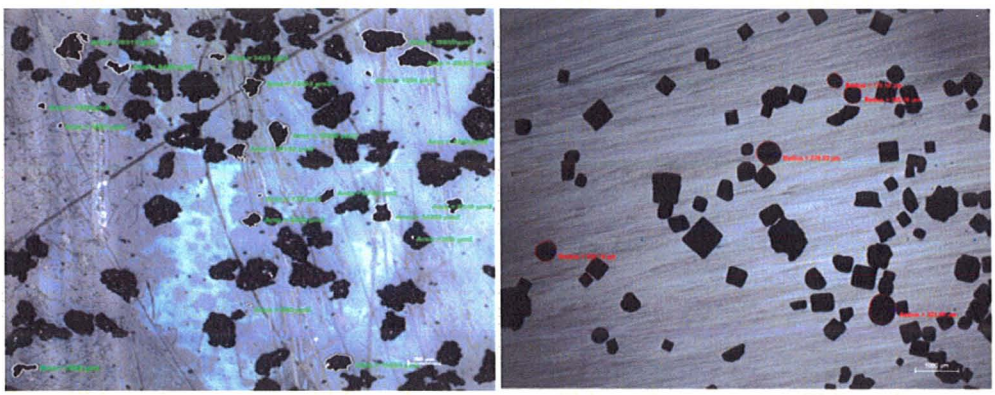

(a) (b)

Figure.3.1. Optical microscope images of (a) ATOMET1001 iron particles and (b) salt particles.

3.2 . Experimental set-up

A versatile and well-instrumented test-rig was designed and fabricated to study the powder filling in a ring-shaped die for a thin high precision component of interest to Gates Canada. The development of this rig was assisted by Dr. Mike Bruhis, Research Engineer in Metal forming Laboratory (MFL) at McMaster University and undergraduate students.

The model die filling system primarily consisted of ring-shaped die, a square shoe, and a pneumatic actuator mounted on a rigid frame. The rigid structure provided excellent stability to the whole rig. A photograph of this system is shown in Fig. 3.2.

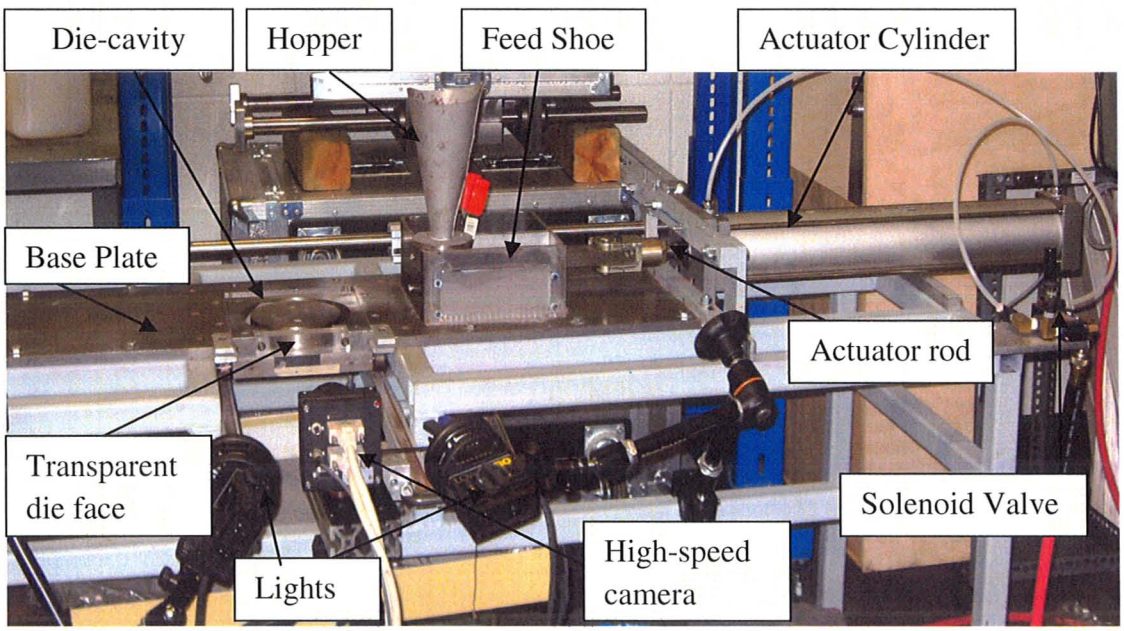

Figure.3.2. Various components of die filling experimental set-up.

The fabrication and function of different components is explained below.

3.2.1. Support frame

A robust steel frame was fabricated by welding to support the die and shoe system with a pneumatic actuator. This frame was fabricated using a heavy steel tubing of 38 mm x 38 mm rectangular cross-section with a wall thickness of 3.175 mm to control any vibrations during the test.

3.2.2. Die-cavity

Die is the most functional part of the system, where the feed-shoe deposits powder during the filling process. The ring-shaped die-cavity with an inner core was machined from cold rolled steel and had a diameter of 152.4 mm. A transparent (Plexiglas) window (or transparent die face) was incorporated on the front side of the die-cavity (Fig. 3.3). The parts were assembled with socket head cap screws. The die could be easily detached from the frame to remove the filled powder or to extract the resin-bonded powder sample from the die without affecting the powder distribution.

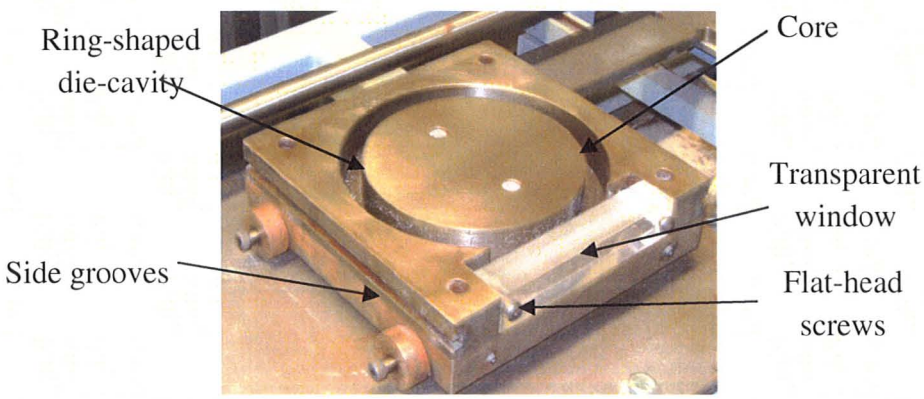

Figure 3.3. Various components of the die-cavity.

Qualitative features of the die:

Two steel plates of size 25.4 mm x 203.4 mm x 196.85 mm were machined down to size by using the end mill cutter. The die was designed and fabricated in three separate parts. The 25.4 mm thick top plate was machined to remove the core part, on the CNC machine, in order to get the shape of the ring. Further, the milling machine was used to drill the holes at specified locations to fasten the top plate to the 25.4 mm bottom plate, and center of the ring together. The rollers were fixed at the bottom of the die, so that the die could be easily rolled on the bottom rails (Fig. 3.3).

Side grooves were machined on to the sides of the die, so that the die could slide over the two rails. Aluminum plates were attached to the underside of the table top surface, on which the die slides to line-up with the table top. With the help of this, die could be easily detached from the steel frame for the heating experiments.

The metal section in the front side of the die-cavity was cut, and a rectangular piece of 24.76 mm x 85.09 mm sheet made out of Plexiglas® was fitted in the die using flat-head screws (Fig. 3.3). The purpose of this window was to record the flow of powder, during the filling process, with the help of a high-speed camera. To get a large area of focus for recording images from the transparent die surface, the inner side of the Plexiglas window was not made into a curved surface. Plexiglas® was chosen as a transparent window because of its good machinability and low cost. A complete die was not feasible because the die was supposed to be heated in the furnace during the resin bonding operation for some of the experiments.

3.2.3. Shoe

A shoe and hopper connected to the shoe are part of the powder delivery system as they deliver the powder into the die-cavity under gravity. In the present work, the shoe was manually filled with powder for many experiments and a small hopper was utilized only for few selected experiments. The actuator rod (driving unit) was connected to the rear shoe-wall which controlled the shoe motion over the die-cavity. The shoe was fabricated from a large cross-section square steel pipe of size 190.5 mm x 190.5 mm with the wall thickness of 6.35 mm. The square pipe was cut down to a length of 100.34 mm on a milling machine using a milling cutter. This pipe when laid vertically made up the walls of the shoe.

Qualitative features:

A rectangular window of 165.1 mm x 62.23 mm was cut from the front side of the shoe, and same size of Plexiglas with a thickness of 6.35 mm was fitted into the shoe using round-head screws. The shoe was divided into two parts with an aluminum plate as shown in Fig. 3.4. Only front portion was filled was filled with powder. This arrangement was made to reduce the amount of powder used during the experiments.

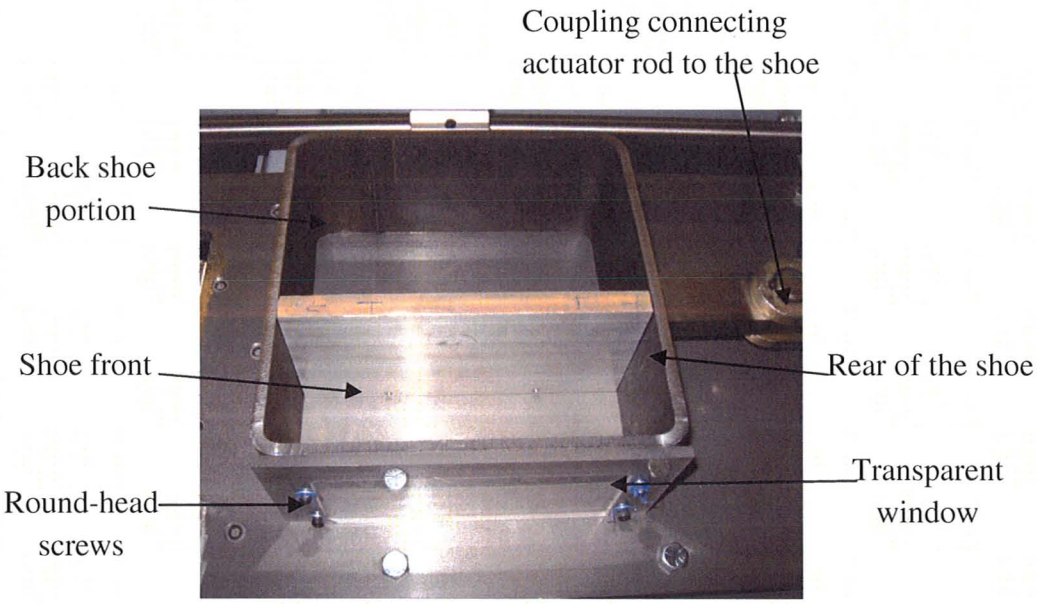

Figure 3.4. Various components of shoe.

3.2.4. Actuation system

A double action pneumatic actuator was selected for this research. The main function of the actuator was to move the powder-filled shoe with a controlled speed. A double action pneumatic cylinder uses pressurized air to move a rod, and the attached shoe on a smooth surface over the die-cavity. The main duct housed in the laboratory was supplied with pressurized air. Air hoses were utilized to bring the air into two ports on the pneumatic cylinder. The flow of the air was controlled with a solenoid valve as shown in Fig. 3.2. A solenoid valve consists of a balanced or easily movable core, which channels air to the appropriate port. Double action cylinder employs the force of air in both forward and retract stroke. Therefore, the actuator rod connected to the shoe could be used to move the shoe forward and backward over the die-cavity.

3.2.5. Hopper

A small conical hopper with an outlet diameter of 50.8 mm was fabricated for a continuous powder supply in the shoe during the filling process for some of the experiments. The extra mass in the small hopper was utilized to study the influence of increased powder level in the front portion of the shoe on the powder flow behavior. The hopper was located over the leading side of the shoe as shown in Fig. 3.5. The hopper was fabricated from two different parts; the top portion cone made of the aluminum sheet joined by welding and base of the hopper was a steel cylinder of inner diameter of 28.2 mm and 50 mm height. Both parts were screwed together.

It is to be noted that due to practical limitations of the room size, the size of the hopper was relatively small in relation to the shoe size compared to the industrial hoppers that are perhaps hundred (or more) times larger than the shoe.

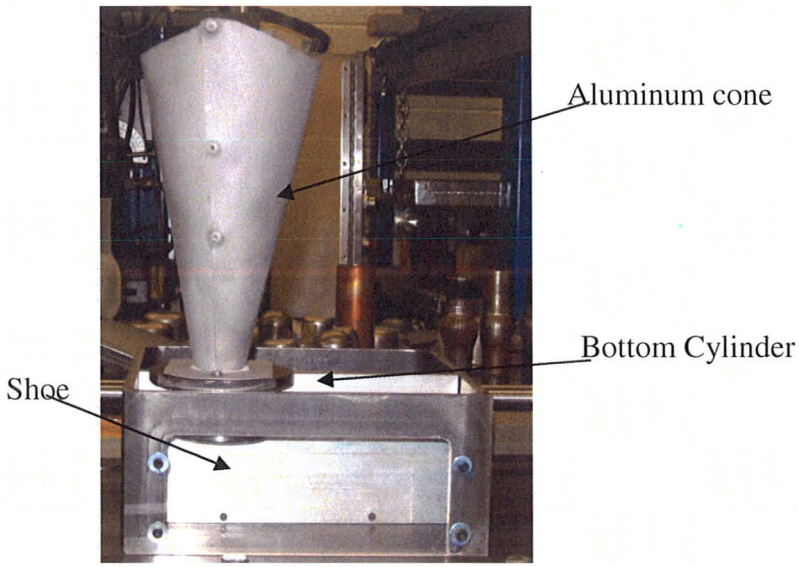

Figure 3.5. Hopper located in front of the shoe.

3.2.6. Perforated plates

Two types of perforated plates were designed and fabricated from an aluminum billet for this research. The billet was machined down to a plate size of 190.5 mm x 59.7 mm using an end mill cutter. The thickness of the plate was 6.35 mm. Perforated plate-1 (or PP1) was created by making periodically spaced straight holes (i.e., perpendicular to the plane of the plate) and perforated plate-2 (PP2) was obtained by tilting the billet between the vise jaw plates after machining the holes. The slant holes in PP2 were machined at an angle of 15^{o} with the vertical axis. The orientation of holes in PP2 was in the backward direction (i.e., towards the trailing side of the shoe) when the perforated plate was placed in the shoe. Holes of 4.06 mm diameter were machined with a spacing of 8 mm as using a programmable CNC machine (See Fig. 3.6). The shoe with the two

perforated plate inserts is referred to as SPP1 or SPP2 in this research and the shoe without the perforated plate insert is referred to as standard shoe (SS).

(a) Perforated plate-1

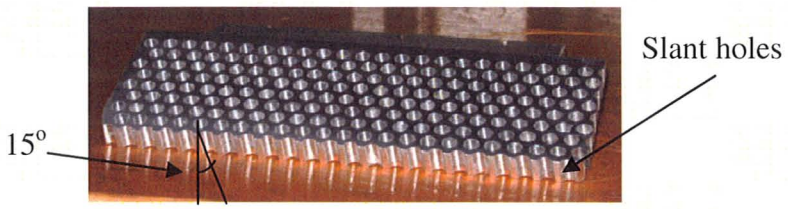

(b) Perforated plate-2

Figure 3.6. Two types of perforated plates used to observe the powder flow.

3.3. Coloured powder die filling experiments

The coloured powder experiments were conducted to easily visualize the macroscopic flow pattern of the powder from SS and SPP1. The effect of perforated plate and shoe velocity on the flow behavior of the powder was examined during gravity die filling. The coloured iron powder and coloured salt powder flow was also compared in terms of different flow patterns and segregation of the powder during the die filling process. The volume of the powder used during the filling experiments was same in all the coloured powder tests except the once with the hopper. All the experiments were carried out at room temperature. In case of iron powder die filling experiments, the iron

powder was heated at 120°C for 1 hour prior to each test to remove any traces of moisture. The salt powder was also dried with fan and stored in an airtight container to avoid moisture.

3.3.1. Tests using coloured salt powder

These die-fill tests were also conducted at room temperature. The salt powder was coloured by using food colours. The filling experiments were performed using tri-layer coloured salt (TLCS) powder bed and tri-column coloured salt (TCCS) powder bed inside the shoe. For the tri-layer pattern, different colours of salt powder were poured one by one manually and leveled with a brush to get three uniform 12 mm thick layers in a 190.5 mm wide shoe. In tri-column pattern of salt powder, three different colour salt powders were poured separately in three equal size columns (i.e., each 63.5 mm thick) and leveled to the same height inside the shoe. Two thin walls (i.e., metal strip) were temporarily placed inside the shoe to separate different colour powder columns. In the presence of the temporary walls and the base plate (below the shoe), the particles then settled to a steady state under gravity as shown in Figs. 3.7a and b. Before starting the experiments, the walls were removed simultaneously without disturbing the leveled columns inside the shoe. Similar arrangement of coloured layers and columns was made in SPP1. Further, the powder flow from the shoe in the die-cavity was continuously recorded with the help of a Canon SX110 digital camera with 9 Megapixel resolution. The filling of coloured salt using SS and SPP1 was analyzed at a shoe velocity of 170 mm/s and 385 mm/s.

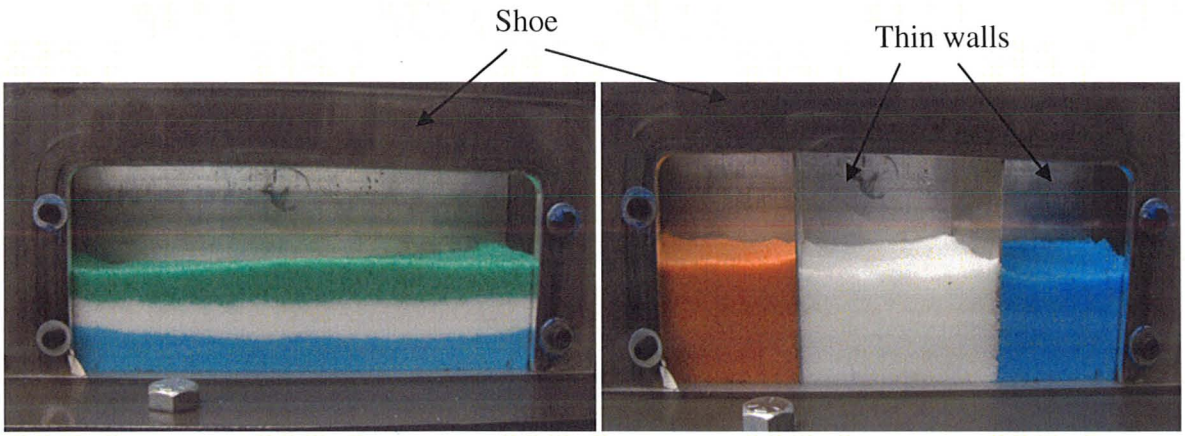

Figure 3.7. Salt powder bed pattern inside the standard shoe, (a) TLCS and (b) TCCS.

Different arrangements (layers and columns) of salt powder were tested for observing and analyzing the segregation pattern and the effective area for powder delivery during the filling process.

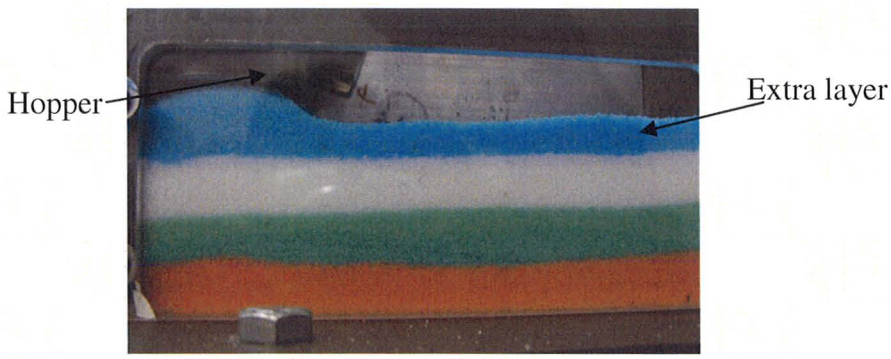

Figure 3.8. Increased salt powder level with an extra mass in the hopper inside SS.

For some experiments, a hopper was placed at the front of the shoe with extra 200 gm of salt and a fourth layer of powder was also added over the top of the standard powder bed (i.e., with three layers) in the shoe (Fig. 3.8). Similar powder arrangement was done in SPP1 in different colours.

3.3.2. Tests using coloured iron powder

Iron powder was coloured by heating it at 180°C for 2 hours in an electric furnace. Powder turned from grey to brown colour due to oxidation of the surface of powder particles. The tri-layer iron powder bed in SS is shown in Fig. 3.9. The arrangement of iron powder was same in SPP1 only the top and bottom layers were brown in colour and the middle layer was grey. The tests on iron powder were performed only in layered pattern using SS and SPP1. The filling experiments were conducted at a shoe velocity of 170 mm/s and 385 mm/s and the flow was recorded with the Canon SX110 digital camera.

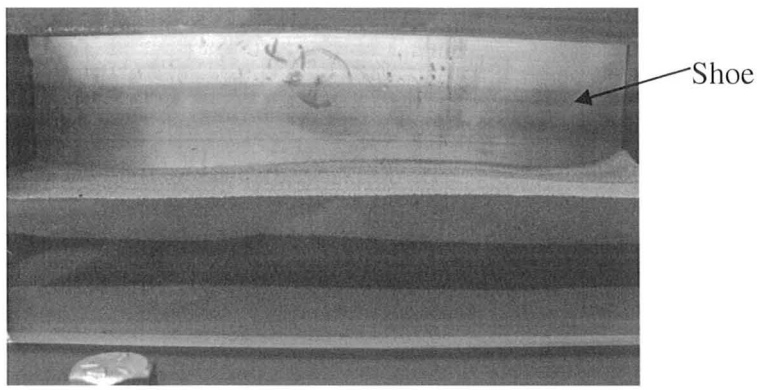

Figure 3.9. Tri-layer iron powder bed inside SS.

3.4. Die filling tests using ARAMIS system

The goal of this study was to investigate the powder flow for a section of ring-shaped die to understand the particle displacement during the filling process, and distribution uniformity at the end of the filling with the ARAMIS system. ARAMIS is a camera-based, online measurement system utilizes a speckle pattern as an image and digital image correlation (DIC) technique to map the displacement field within the imaged region from a series of images during the test.

For particle displacement tracking through ARAMIS system, powder flow from SS, SPP1, and SPP2 were recorded. Fig. 3.2 presented earlier showed the experimental set-up of die-fill system with a CCD camera. In these experiments, shoe with a hopper was traversed over the die-cavity at a velocity of 170 mm/s with the pneumatic actuator system. The powder was delivered under gravity into the die. The hopper filled with powder was mounted over the leading side of the shoe to supply additional powder to the shoe. Then, the images were recorded with the help of high-speed camera for different stages of the filling process. The powder flow through the shoe and die-cavity was monitored closely during the filling process with the high-speed camera images.

All tests using ARAMIS were performed at a shoe velocity of 170 mm/s, using iron powder. In addition, when using ARAMIS, Plexiglas® window incorporated in the die was cleaned with a liquid solution before every test. The purpose of cleaning was to remove the fine scratches, dirt, and static charge from the Plexiglas® surface, so that the

clear powder images could be recorded through the window. ARAMIS results were analyzed in terms of displacement contours for different stages of filling (Section 4.6).

3.4.1. Camera set-up and recording conditions

The ARAMIS system uses DIC method to calculate the displacement of particles during the die-filling process at different stages. The displacement data can be used to understand the filling operation and settling time of the powder, when the powder drops from the shoe into the die. A Schneider CCD-1300BG camera, a part of the ARAMIS system, captured a series of images during the die-filling process through the Plexiglas window. The time gap between the end of forward stroke and the start of retraction of the filling process was 5 sec. In addition, two light sources were utilized to illuminate the die-cavity uniformly for recording good quality images (See Fig. 3.2). The light during image recording, needed to be proficient, to eliminate errors in the calculations due to faulty image quality. During the die-filling, images of the powder, moving with high speed, were recorded after designated time intervals. The CCD camera was controlled by the ARAMIS software and was placed directly in front of the transparent window. The images are recorded at the rate of 300 frames per second (fps). The shutter time of the lens is set to 3.16 ms. Camera was mounted on a tripod so that the focus could be adjusted to see the whole die-cavity window without disturbing the camera position.

3.4.2. Digital Image Correlation (DIC) method for displacement calculation

Digital Image Correlation is a full-field image analysis method, based on grey value digital images that employ tracking and image registration techniques for accurate 2D and 3D measurements of deformation, displacement, and strain from the digital

images. In this research, the DIC method is used to analyze the dynamic behavior of metal powder depositing into a ring-shape die-cavity. The calculation was done based on a rectangular facet or network of points which deform between images at different filling stages. The technique allows for tracking particle movement at any desired point in the imaged 2D powder field. For a more detailed description of the general DIC method, the reader is referred to Verhulp et al., 2004.

3.5. Procedure for determining filling rate

The filling rate of a powder is the ratio of total mass of powder filled into the die-cavity to the filling time (Wu et al., 2003). During the filling stage, the mass transferred into the die after a forward pass of the shoe was measured with the Wei-Heng series electronic weighing balance for iron powder. The filling time was determined by measuring the total time required, using a stop watch, for the shoe filled with powder to translate from the initial position to the final position (i.e., when it comes to rest after the forward pass) on the base plate during filling. The filling rate study was performed using SS and SPP1, with and without the hopper. The experiment was repeated three times for each condition to obtain accurate filling rate data.

3.6. Iron powder binding after die filling process

The purpose of binding iron particles in die-fill condition was to analyze the density distribution in different locations of the die with the help of Gamma ray densitometry. This was achieved by mixing the iron powder with a polymer (polyethylene) resin and heating the mixture at a low temperature of 195^{o}C without disturbing the particle distribution in the die. This process is similar to sintering of a

green compact where a coherent bonded mass is formed by heating metallic or nonmetallic powders below the melting point of the powder material. The mixing of polyethylene and iron powders was performed in a ball mill. The blend of the iron powder with 10% polymer powder was made without affecting its flow-ability. Ceramic balls of different diameters were used as a mixing media. A plastic bottle was partially filled with powder mixture and the alumina balls and placed in the ball mill. The rollers of the ball mill were rotated along their axis at a speed of 126 rpm (Fig. 3.10). A significant effort was made to refine the powder heating method and to optimize the temperature required to bond the high density polyethylene (HDPE) particles, rate of heating, holding time for the part to get a uniform bonding and without boiling the liquid polymer. The goal of binding the iron particles deposited in the die by ex-situ heating was achieved. By mixing the polyethylene resin, the sintering temperature of the filled power was reduced to the melting temperature (195^{o}C) of the polyethylene powder.

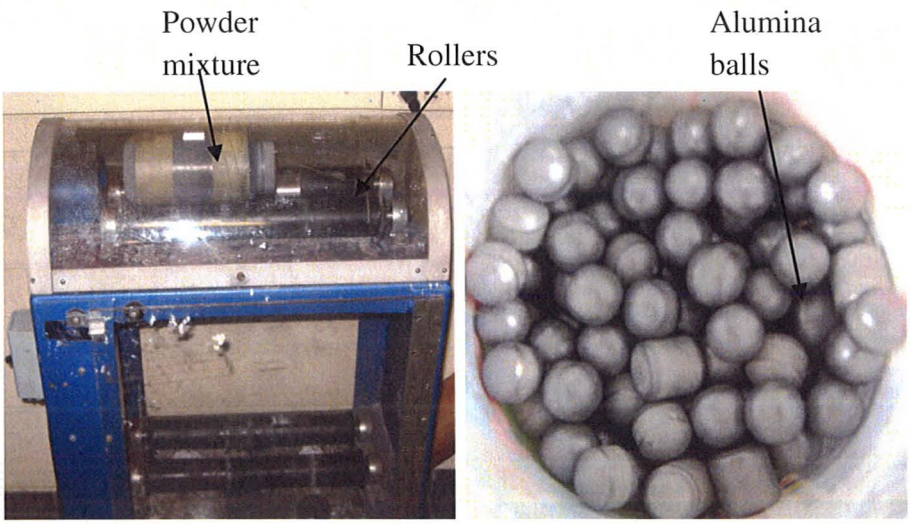

Figure 3.10. Mixing of iron powder and polyethylene powder in the ball mill.

The mixture extracted from the ball mill was poured into the shoe and then delivered to the die. For this heating experiment, the die top plate with a Plexiglas® window was changed with the complete steel plate. The die was slowly removed form the table frame and placed inside the furnace and covered from the top with a Mylar sheet. The temperature of the furnace was set to 195°C with a heating rate of 5.5°/min. The sample was held at 195°C for 90 min. Further, the die with iron powder sample was furnace cooled to room temperature. During powder heating, the liquid resin flows into the inter-particle space to create a strong bonding. The choice of polyethylene was based on its melting point and other physical properties. Samples were obtained for both SS filling and SPP1 filling process.

The samples were removed from the die and carefully sectioned along the circumference of the ring-shaped part to measure the density in different locations. The volume was calculated by measuring the length, breadth, and thickness of the cut-section using a caliper. Further, the samples were taken to the gamma densitometry and attenuated gamma ray counts for all samples were recorded (Section 3.8.2).

3.7. Powder property measurement techniques

3.7.1. Bulk density measurement

The bulk density of a powder is the weight of the powder divided by the volume it occupies, normally expressed as g/ml or kg/l. It was calculated by a simple measurement technique that included a 100 ml glass measuring cylinder and a Wei-Heng series electronic weigh scale. The powder was poured using a funnel inside the entire volume of the cylinder without shaking or tapping it and removing any excess powder from the top

electronic weigh scale. The powder was poured using a funnel inside the entire volume of the cylinder without shaking or tapping it and removing any excess powder from the top of the cylinder. The powder filled cylinder was then placed on the weight-scale to determine the mass of the powder. This test was repeated five times for each powder to get the accurate bulk density values.

3.7.2. Angle of Repose

Angle of repose is a characteristic of powder material which depends on the friction between the particulate matters. It is defined as the angle made by a slope of the pile of powder with the base. Angle of repose is constant and a three dimensional angle relative to the horizontal. Dynamic angle of repose is the angle (relative to the horizontal) formed by flowing powder. The powders with lower angle of repose show good flow-ability than the powders with higher angle of repose.

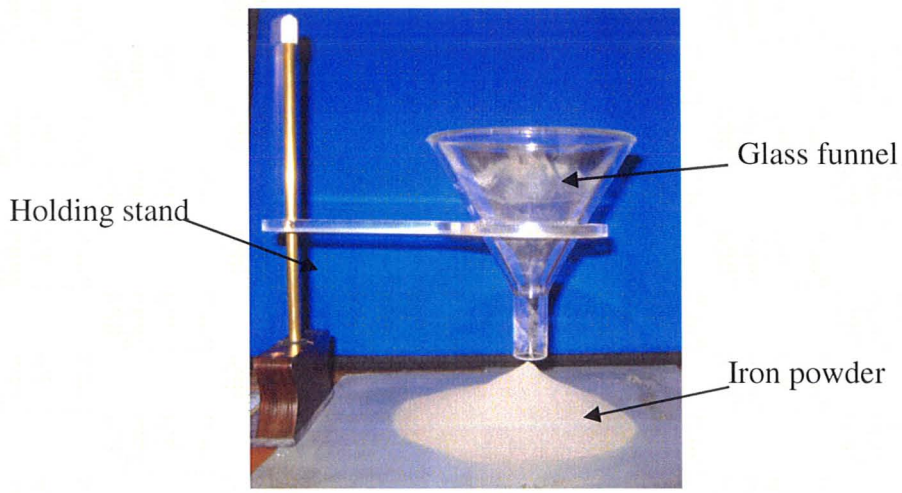

Figure 3.11. Angle of repose measurement set-up.

and a base. The height of the funnel outlet above the base was adjusted to 3 mm. Further, the base of the funnel outlet was covered with a metal strip and 100 ml of powder (iron or salt) was filled in the funnel. The strip was released, and powder was allowed to fall freely onto the base. The angle which the stable powder heap makes the horizontal base is the angle of repose. Angle of repose for iron and salt powders was measured using an angle measuring tool from the Autodesk Inventor software on the recorded images. The static angle of repose for iron was between 20^{o}-23^{o}, and for salt powder between 26-29^{o}. Dynamic angle of repose was calculated by capturing the high quality images during the flow with the high-speed camera and an angle measuring tool from the Autodesk Inventor. This test was repeated three times for each powder to get the accurate angle of repose.

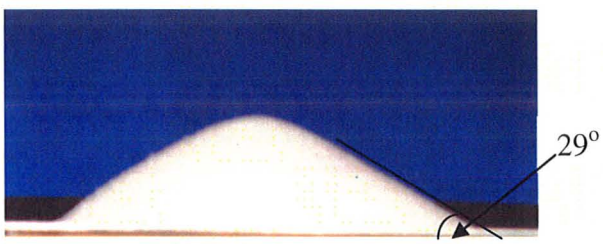

Figure 3.12. Angle of repose for salt powder.

3.8. Density measurement of heated sample

The die fill density of the resin-bonded sample was calculated from two different methods; mass and volume measurement and Gamma ray densitometry.

3.8.1 Mass and volume

After filling, powder mixture in the die-cavity was heated, and sections from different locations of the ring-shaped part were cut using a saw cutter and weighed. Mass of each sample was measured using calibrated Acculab digital lab scale VIC-212. Density of a material is the ratio of mass of the material to the volume of the material. The volume of rectangular parallelepiped resin-bonded iron sample was obtained by measuring (in mm) the length (L), width (w) and thickness (t) of each part using a caliper. This procedure was repeated three times to find an average density value.

3.8.2 Gamma ray densitometry

This technique is based on the exponential decrease in the intensity of collimated beam of gamma rays as it passes through the matter. The attenuation of the electromagnetic gamma-radiation in matter leads to a loss of intensity. As the attenuation, in solids and liquids is higher than in gases, the loss of intensity is a means to conclude on the phase of matter, which is crossed by a gamma-beam. The unscattered gamma ray intensity after passing through a material depends on the atomic number of the material, thickness of the sample, and the density of the part. This non-destructive method is useful de assessing the density uniformity in components. The main advantage of gamma densitometry is that a thicker sample can be tested efficiently due to high-penetration

energy of γ-rays compared to X-rays. Further, gamma rays can spread in all directions; thus, full sample can be tested at once.

A gamma ray densitometry set-up in the Department of Engineering Physics at McMaster University consisted of an americium-241 gamma source (gamma ray energy of 60 KeV), a sodium iodide scintillating device and a multichannel analyzer. This set-up provided the volume averaged void fraction of various resin-bonded powder samples. The γ-ray source is radio-nuclide, which emits in its decay process mono-energetic photons called gamma radiation. The gamma rays are passed through the material, and from the other end, the transmitted radiations are counted, using a multichannel analyzer in pulse height analysis mode. The count rate time was set to 60 sec to measure the accuracy of ε_g (void fraction).

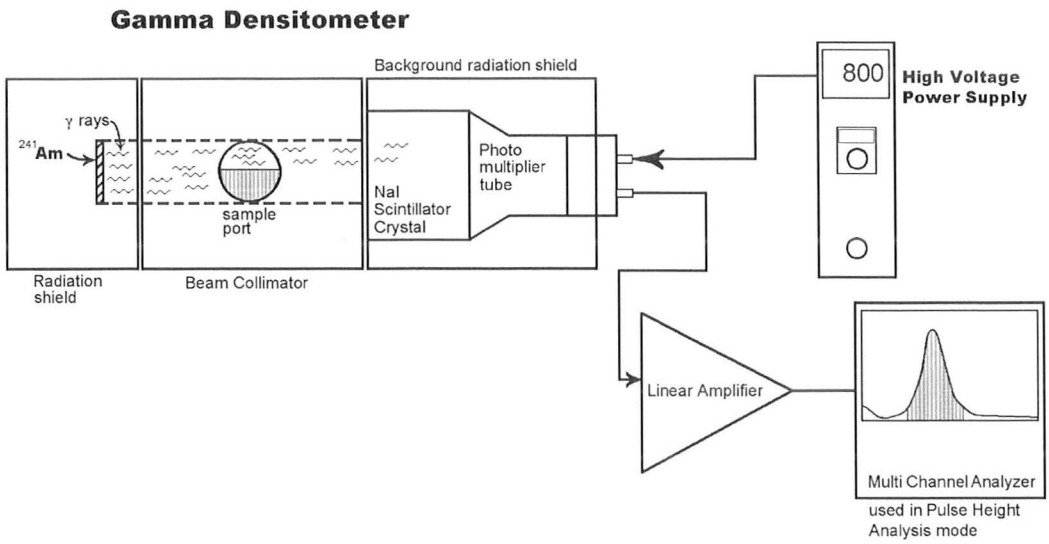

Figure 3.13. Schematic of Gamma ray densitometer two phase flow experimental set-up.

The void fraction of a sample was calculated by using the following formula:

$$\varepsilon_g = \frac{\ell n\left[N_{(\varepsilon_g=0)} / N_{\varepsilon_g}\right]}{\ell n\left[N_{(\varepsilon_g=0)} / N_{(\varepsilon_g=1)}\right]}$$

where, N (ε_g =0), N(ε_g =1), are the two extremes values corresponding to count rates of a zero void and unit void respectively and N(ε_g) the void count to be measured for the test sample. The full-energy peak, which corresponded to the unscattered gamma rays, was compared with the output from the test samples, to obtain the void fraction of the test sample. The powder samples bound together with resin were analyzed with gamma ray densitometry, to get die-fill density distribution data.

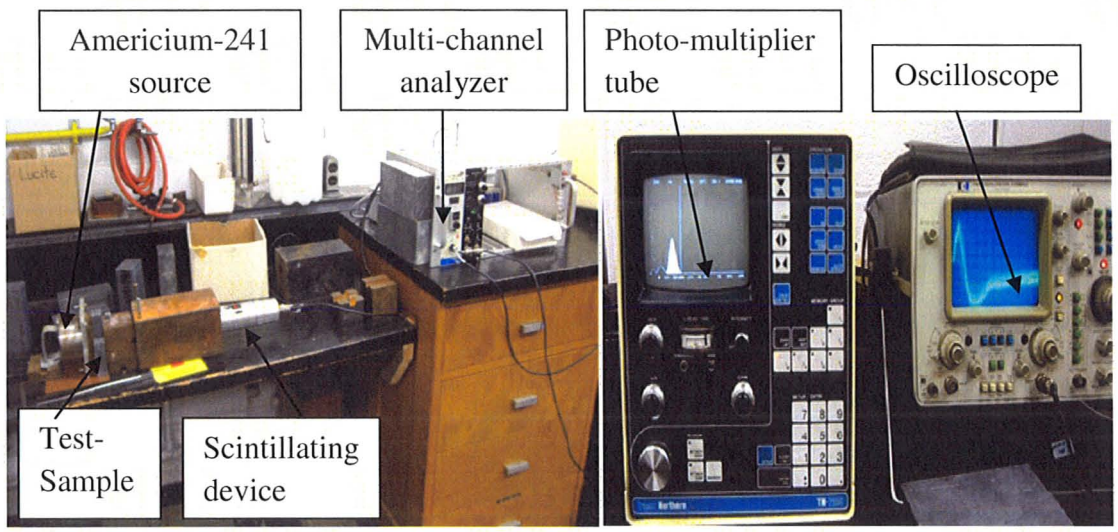

Figure 3.14. Laboratory gamma ray densitometry set-up.

The linear attenuation coefficient of iron is 2.72, whereas carbon is 0.335 as recorded by NIST (Physical measurement laboratory), USA. It is evident that, the scattering of the gamma rays is affected by the atomic number of the test material. Thus, the absorption of the gamma rays by polyethylene powder was expected to be lesser than the iron powder, as polyethylene is composed of carbon and hydrogen molecules.

3.8.3. Determination of surface porosity by image analysis

The NIS- Element BR-3-0 image analysis software was utilized to measure the surface porosity distribution from the recorded images from the transparent die face (TDF) section at the end of the filling process. A pixel classifier within the software defined the areas of the image which were identified as pore space (Parker, 1991). Each pixel in the image was justified either a pore space or a grain space by comparing the brightness of the pixel to a selected threshold level. This threshold method was based on the assumption that all pixels brighter than the threshold value were part of the grain space, and all pixels darker than the threshold value were part of the pore space. The drawback of this technique is that the threshold value is determined by trial and error and may not accurately distinguish pore space from the grain space in the image. If the image contains dark grains, which reflect or transmit, less light than the pore space, the threshold technique may erroneously consider the dark or nonreflecting grains as pore space. A satisfactory bi-level image could not be obtained when the illumination gradient was large. A single threshold for all images did not work well.

The measurement of surface porosity on the TDF was performed by recording the image of the powder at the end of the filling process (Fig. 3.15). The shoe with a hopper was moved to forward and backward over the die-cavity during the filling process. The hopper helped in eliminating the depression from the front of the shoe during shoe motion. In order to measure the repeatability of porosity distribution for two different filling methods (SS and SPP1), 8 filling tests for each point were conducted while reading the images of the final stage. The porosity measurements were rather sensitive to the light conditions during image capture; a uniform lighting with a high-speed camera was utilized in all experiments to get consistent results.

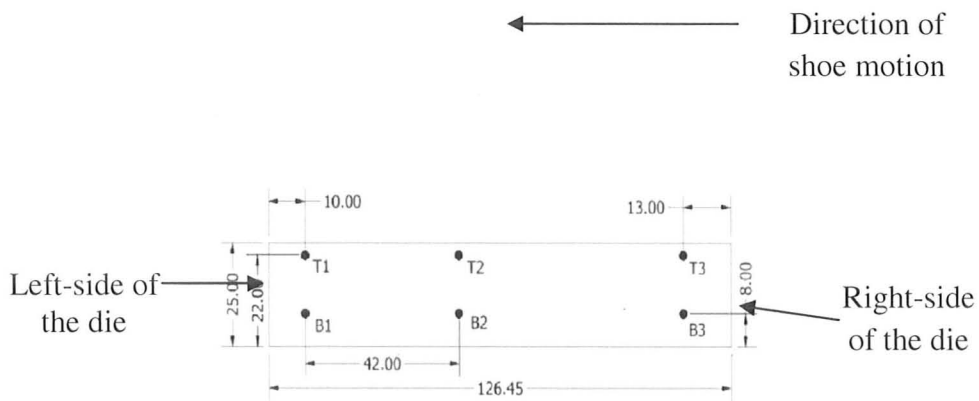

Figure 3.15. View of six point locations on the transparent die face.

Fig 3.16 shows the pore space and grain space in the iron powder recorded during the filling process.

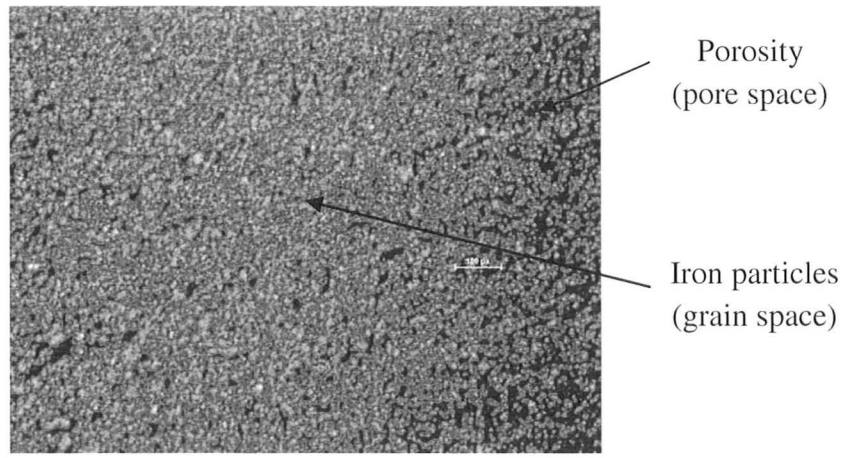

Figure 3.16. Image showing porosity and iron particles after image analysis.

Images of raw iron powder in die-fill stage had some illumination gradient, for rectifying its effect on porosity analysis; all reasonable thresholds were applied to the image under observation and then correlated with the original image. The threshold value producing a satisfactory bi-level image was selected, by identifying pore and iron particle pixels, after performing the iterations.

CHAPTER 4

EXPERIMENTAL RESULTS AND ANALYSIS

4.1. Types of Flow

The die filling experiments using tri-layer coloured salt (TLCS) powder bed were conducted to assess the macroscopic flow pattern of particles during the forward pass of the filling process. Coloured salt was used as a powder medium in these tests. Three equal-sized layers of coloured powder were filled inside the feed-shoe. The powder bed comprised of salt powder of the same particle size and density but differently coloured.

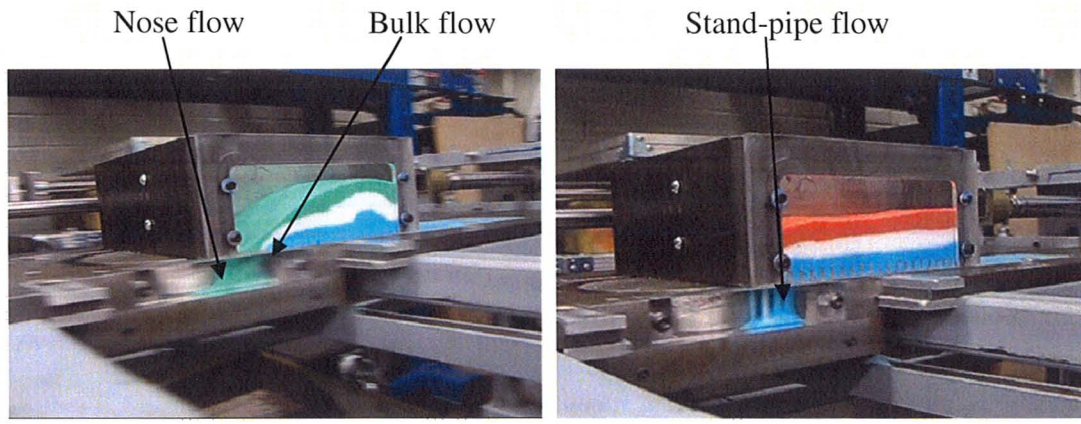

Figure 4.1. Types of flow in die filling process using a) SS and b) SPP1.

Three types of powder flow were observed as shown in Figs. 4.1a and b for a shoe moving at a speed of 385 mm/s. During die filling with a standard shoe, powder moves back towards the wall of the shoe, forming a nose shaped profile inside the shoe, and the powder from the upper surface of the nose flows rapidly into the die creating a gap between the die wall and the front stream of powder. This flow is referred to as nose flow as shown in Fig. 4.1a. As the shoe traverses over the die cavity, particles from the bottom layer of the powder mass detach into the die-cavity, which is known as bulk flow of powder. The bottom blue-layer particles in Fig. 4.1a represent the bulk flow into the die-cavity. During die filling using SPP1, powder flow is in small segments through the holes, straight into the die-cavity, as shown in Fig. 4.1b. This type of flow is referred as standpipe flow in this thesis. In addition, in SS a large gap (depression) is created in front of the shoe, whereas in SPP1, the powder level in the front slightly moves down. The uneven distribution of powder in the standard shoe applies diverse packing pressure on the powder in the die-cavity, which results in nonuniform packing of powder in left and right-side of the die-cavity.

It can be noted that with the standard shoe mass flow of powder takes place into the die-cavity, whereas with the use of perforated plate (SPP1) the bulk of powder mass is broken down into small segments, and a free flow of the powder is observed. Thus, a controlled flow is achieved with SPP1. A more detailed analysis of segregation of powder during die filling is presented in Section 4.2.

4.2. Coloured powder flow behavior analysis

In this section, further analysis of the coloured powder flow behavior is presented with the focus on the effect of shoe velocity on powder segregation and particle packing in the die-cavity during filling.

4.2.1. Die filling with TLCS powder bed using SS

The effect of shoe velocity on the powder flow from a standard shoe is described in this section. The snapshots of die filling with TLCS powder at a shoe velocity of 170mm/s are shown in Fig. 4.2.

As the shoe accelerate from the rest, powder moves to the back of the shoe due to the combined effect of inertia and the frictional sliding between the bottom of the powder mass and the base plate. All the three layers slightly deform and pack towards the rear of the shoe, and a post-avalanche angle of 38^{o} is formed in the powder mass in front of the shoe (Fig. 4.2d). As a result, a gap is formed at the front of the shoe, which grows as the shoe translates. In the initial stage of filling, powder cascades from the topmost layer of the powder mass into the die and deposits first in the bottom of the die (Fig. 4.2b). This creates a nose flow, which is consistent, with the analysis of Wu et al., (2003a). Fig. 4.2c shows the intermediate stage of the filling process, where SS comes partially over the die, and particles from the bottom surface of the shoe detach into the die-cavity. Flow rate of the powder mass from the bottom of the shoe is more as the shoe velocity is low; therefore, thick layer of blue colour particles is deposited in the top region of the die. As a result, the top region of the cavity is filled by the bottom layer of the powder mass. In the intermediate stages of filling, segregation of the middle layer particles occur just

before the bottom layer particles fall into the die-cavity. A thin layer of white particles is formed between the top and bottom layer in the die (Fig. 4.2c). The mixing of the white particles with the top and bottom layer particles inside the die occurs due to particle rearrangement in the die during the filling process (Fig. 4.2e). Both nose flow and bulk flow contribute to the filling process at a shoe velocity of 170 mm/s.

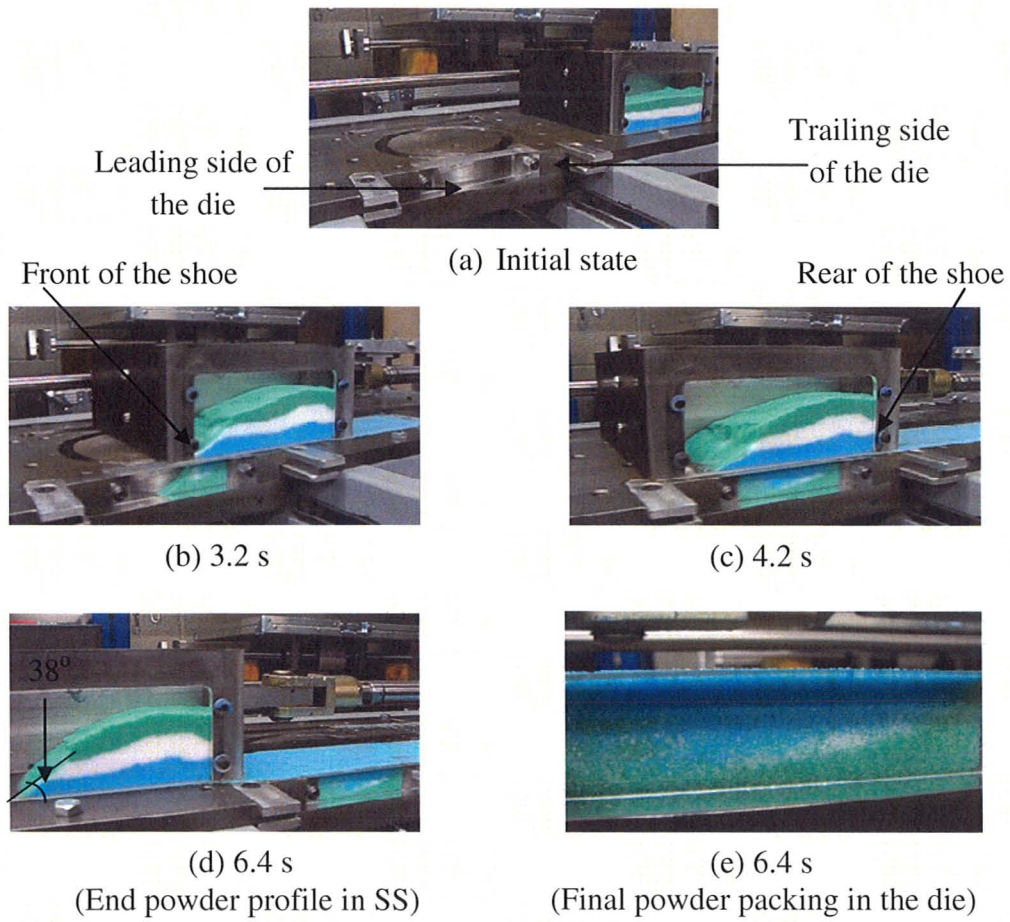

Figure 4.2. Powder flow pattern with TLCS powder bed at different times during the shoe motion, using SS (V_{shoe}= 170 mm/s).

Results at a velocity of 385 mm/s are presented in Fig. 4.3. At this higher shoe velocity, the powder layer mixture, inside the shoe, deforms to a greater extent and rises along the shoe-wall. A slope in the entire powder mass is formed inside the shoe, which accelerates more particles from the top free surface into the die (Fig. 4.3a). Fig. 4.3c shows a post-avalanche angle of 31^{o} at the end of the forward stroke in the shoe. The post-avalanche angle represents the static angle of repose of the powder and correlates to the quantity of avalanched mass [Lavoie et al., 2002]. The angle obtained at a shoe velocity of 170 mm/s with TLCS powder bed using SS is greater than the angle obtained at a velocity of 385 mm/s which means the powder flow-ability inside the shoe is better at higher velocity. A severe rotational flow during rearrangement of particles is observed inside the powder mass during the shoe motion. Final packing of the powder in the die shows, as earlier, a reversed pattern of layers inside the die-cavity (Fig. 4.3d). It can be seen that the top and middle layer particles are accelerated more than the bottom particles, and therefore, deliver the majority of the powder to the die. At this higher shoe velocity, the particle detachment during the bulk flow is less due to the combined effect of entrapped air and interlocking of the particles. This condition creates a thinner band of blue particles at the top of the die-cavity compared to the shoe velocity of 170 mm/s (Fig. 4.3d).

It can be noted that segregation sequence of the powder layers is similar to that observed in lower shoe velocity, but the amount of powder deposited from different layers, during die filling, differs in the two cases. Also, the powder mass inside the shoe changes its profile (layers rearrangement) significantly at a shoe velocity of 385 mm/s,

whereas powder mass inside the shoe deforms very little at 170 mm/s (Figs. 4.2d and 4.3c). It is also clear that powder flows with more intensity at high shoe velocity and fills the die quickly.

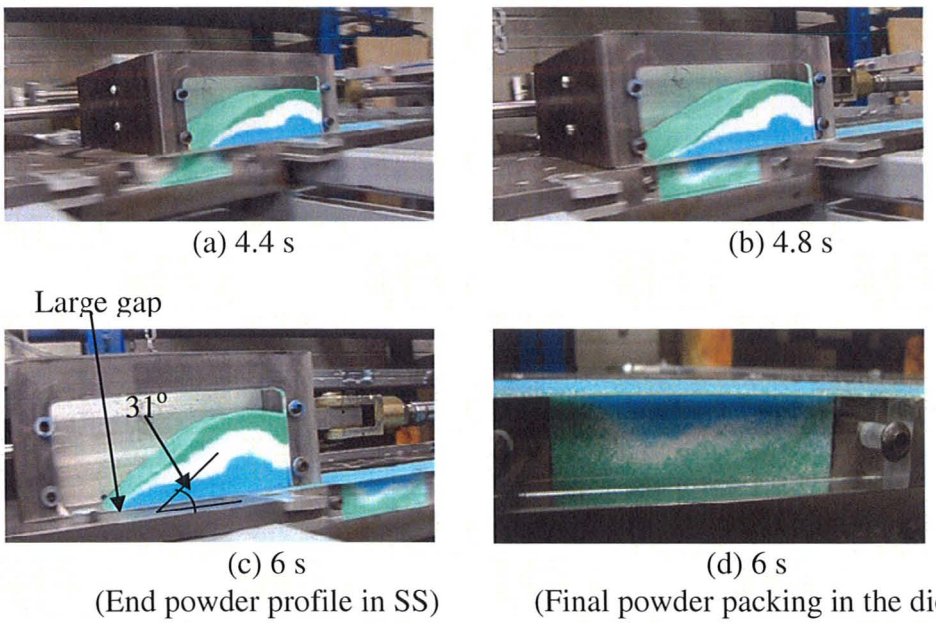

(a) 4.4 s (b) 4.8 s

(c) 6 s (End powder profile in SS) (d) 6 s (Final powder packing in the die)

Figure.4.3. Powder flow pattern with TLCS powder bed at different times during the shoe motion, using SS (V_{shoe}=385 mm/s).

4.2.2. Die filling with TLCS powder bed using SPP1

The results of powder flow patterns at a shoe velocity of 385 mm/s using SPP1 are presented in Fig. 4.4. The initial arrangement of TLCS powder is similar to that in the previous section; only top layer colour has been changed from green to red (Fig. 4.4a). The powder profile in the shoe and the final particle packing in the die were found to be similar at 170 mm/s and 385 mm/s; thus, only segregation results at 385 mm/s are presented in this section. The shoe powder profile at the end of the forward pass shows

no significant rearrangement of powder layers during shoe motion, which means that the motion of powder is confined between the bottom of the shoe and in the vicinity of the perforated plate (Fig. 4.4d). A post-avalanche angle of approximately 20^{o} in the top surface of the powder bed is obtained, which is significantly smaller than the static angle of repose calculated for salt powder (Section 3.7.2). This is due to the change in the degree of aeration in the powder mass during the avalanche.

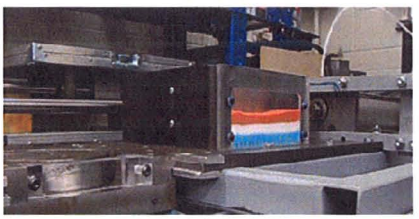

(a) Initial state

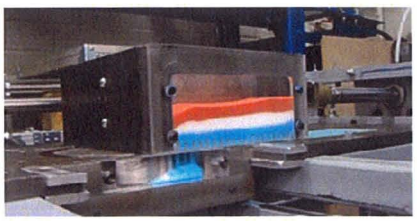

(b) 3.1 s

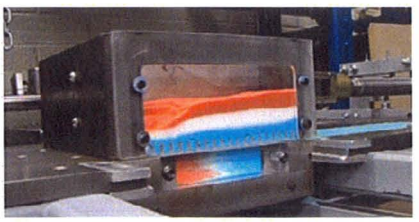

(c) 4 s

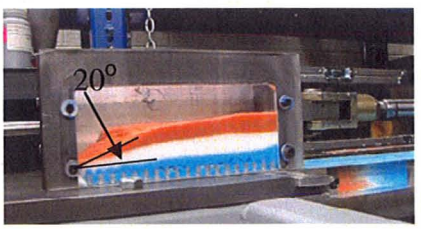

(d) 6.2 s
(End powder profile in SPP1)

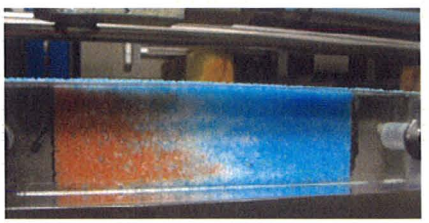

(e) 6.2 s
(Final powder packing in the die)

Figure 4.4. Powder flow patterns of TLCS powder bed at different times during the shoe motion, using SPP1 (V_{shoe}= 385 mm/s).

In the initial stage of the filling process, it can be seen that the powder flows vertically in a controlled manner through the holes in the perforated plate into the die. At first, the bottom layer particles are delivered from the front stream of the powder mass into the right-side of the die-cavity. Further, as the shoe translates over the die dropping the middle layer (coloured in white) particles flow through the holes in front of the perforated plate into the middle portion of the die-cavity. At the end of forward stroke of the filling process, front portion holes in the perforated plate are refilled by the particles from the top layer of the shoe. Consequently, the top layer (coloured in red) cascades down the small slope through the holes into the die-cavity (Fig. 4.4c). Further, the red colour particles deposit on the left-side of the die-cavity. The final packing of powder in the die illustrates that mainly front stream of powder mass (i.e., leading side of the shoe) pours powder into the cavity, and the powder mass near the rear end of the shoe deposited significantly less into the die-cavity.

It can be noted that TLCS powder sequence in the shoe converts into tri-column powder bed (TCCS) inside the die-cavity (Fig. 4.4e), at the end of the filling process, whereas in the case of the earlier powder filling with SS, the sequence of TLCS bed inside the shoe is reversed in the die-cavity (Fig. 4.3d). This illustrates a different pattern of segregation of powder through the perforated plate during different stages of filling compared to the standard shoe.

4.2.3. Die filling with TCCS powder bed

In this section, die filling with tri-column coloured salt powder bed using SS and SPP1 are reported.

4.2.3.1. Die Filling using SS

Fig. 4.5 describes the flow behavior of powder during die filling with a tri-column coloured powder (TCCP) mixture inside the standard shoe at a shoe velocity of 170 mm/s. The initial arrangement of coloured powder mass is shown in Fig. 4.5a. At first, the left column of the powder mass (coloured in red) moves slowly over the die-cavity. The other two columns (coloured in white and blue) do not accelerate to a greater extent, and slightly move back towards the shoe-wall (Fig. 4.5c). As a result, the entire filling takes place from the front column particles. The post-avalanche angle of 35^{o} in front portion of the shoe is obtained as shown in Fig. 4.5d. The difference in the post-avalanche angle for TLCS and TCCS powder bed using SS is because of the initial arrangement of powder in the shoe as explained in Section 3.3.1. When the salt powder is poured in the shoe, the powder bed containing different size particles segregate under gravity and as a result, smaller particles sink to the bottom of the shoe and larger particles remain at the top. Thus, the flow patterns of the powder vary during the filling process.

(a) Initial state

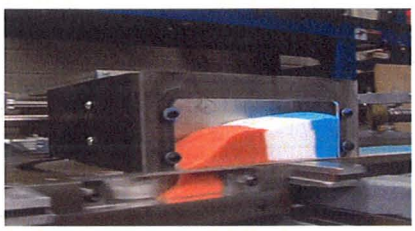

(b) 5.1 s

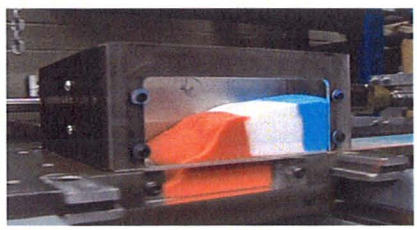

(c) 5.4 s

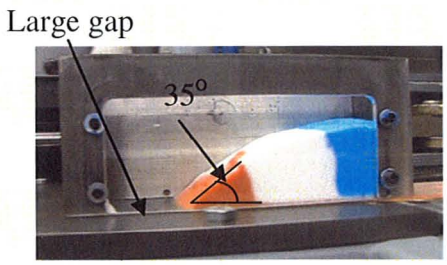

(d) 7 s
(End powder profile in SS)

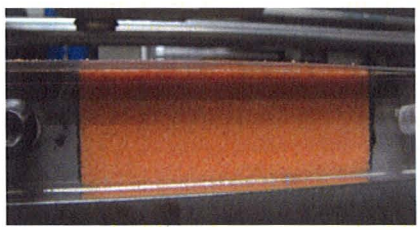

(e) 7 s
(Final powder packing in the die)

Figure 4.5. Powder flow patterns during die filling with TLCS powder bed at different times of the shoe motion, using SS (V_{shoe} =170 mm/s).

During die filling at a shoe velocity of 385mm/s, initial arrangement of powder bed inside the SS is similar to that shown in Fig. 4.5a. It can be seen that as the powder moves back in the moving shoe with higher intensity, all the three columns move to form a nose shaped profile in the shoe. This makes the middle column particles (coloured in white) to avalanche down the slope into a small portion towards the left-side of the die-cavity. This occurs after the top left column has filled major portion of the cavity (Fig.

4.6d). A post-avalanche angle of 27° is observed in the powder mass inside the shoe at the end of the first pass (Fig. 4.6c), which is smaller than the angle obtained at a shoe velocity of 170 mm/s with TCCS powder bed using SS. This means the powder shows better flow-ability at higher shoe velocity (Section 3.7.2). The gap created in front of the shoe depends on the amount of powder inside the shoe and the shoe velocity. The final particle packing inside the die-cavity shows particles from left and middle columns of the powder mixture. The particles from the right column do not contribute to the filling because by the time right column start to cascade down the slope the shoe comes to rest.

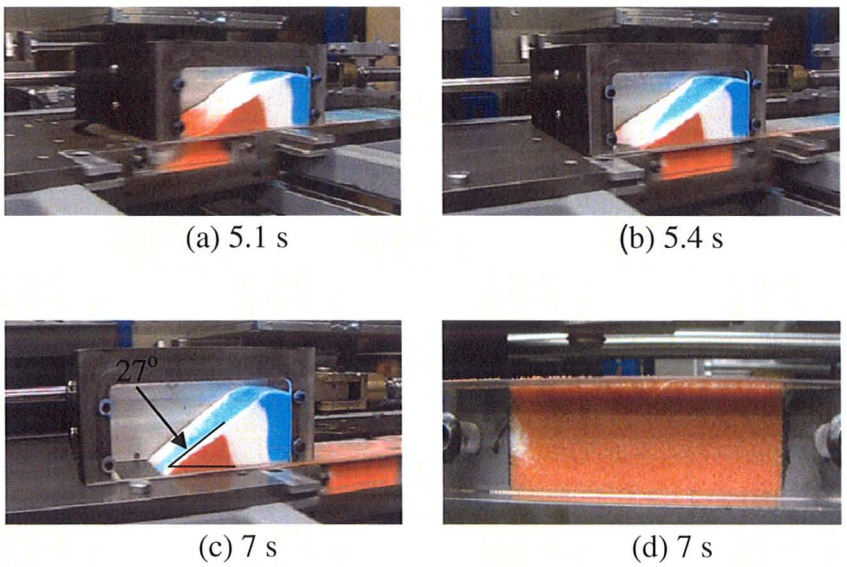

(a) 5.1 s (b) 5.4 s

(c) 7 s (d) 7 s

Figure 4.6. Powder flow patterns with TCS bed at different times of the shoe motion, using SS (V_{shoe} =385mm/s).

4.2.3.2. Die filling with SPP1

Fig. 4.7 describes the powder flow behavior during die filling with a TCCS powder bed using SPP1 at different shoe velocities. The arrangement of the coloured

powder mixture inside the shoe is similar to the previous section. It is noted that, at a shoe velocity of 170 mm/s, tri-column mixture delivers the powder entirely from the left column, as shown in Case I, Fig. 4.7d. Thus, the final powder packing in the die shows only front column particles. The final profile of the powder bed in the shoe shows a depression in the left column of the shoe, but the other two columns show negligible change (Fig. 4.7c). The post-avalanche angle observed is 20^{o} in the front, which is same as obtained in the earlier case of SPP1 with tri-layer salt powder bed due to the initial arrangement of the salt powder bed inside the shoe.

In Case II, Fig. 4.7, it can be seen that powder column displaces slightly even at shoe velocity of 385mm/s. A small slope of 10^{o} at the front column of powder bed inside the shoe is created. At this velocity, it can be seen that the first column particles (left-side of the shoe) moves quickly over the die-cavity leaving the top region of the cavity empty. As a result, the middle column (coloured in blue) of the powder mass fills the space in the top region of the cavity (Fig. 4.7h). Fig. 4.7i shows the final packing of the powder inside the die.

It is clear that, with the use of a perforated plate, the shoe velocity shows very little impact on the rearrangement of powder inside the shoe after the first pass of the filling process, whereas the powder profile inside the SS changes significantly with the shoe velocity. It is evident that the avalanche flow increases the aeration in the powder mass in SS. Therefore, the final particle distributions inside the die-cavity are different in the two cases (SS and SPP1).

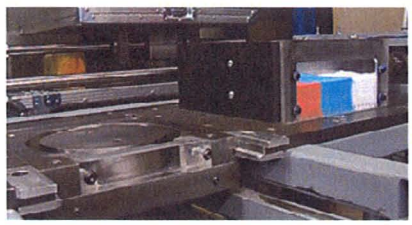

(I) (a) Initial position

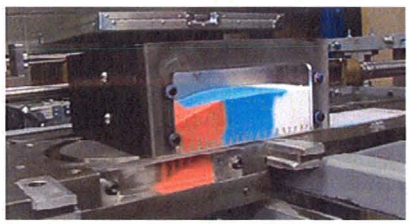

(b) 2.9 s

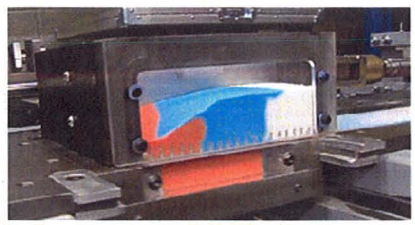

(c) 3.5 s

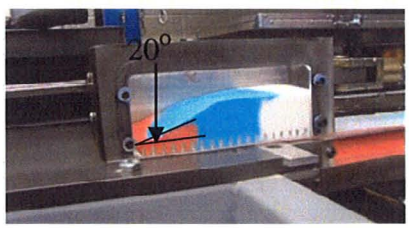

(d) 5.5 s

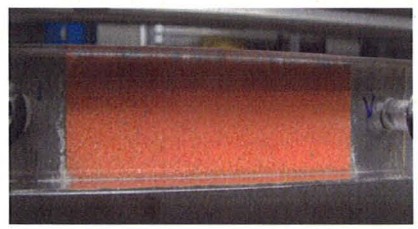

(e) 5.5 s

(II)

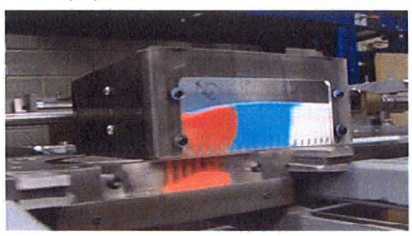

(f) 2.4 s

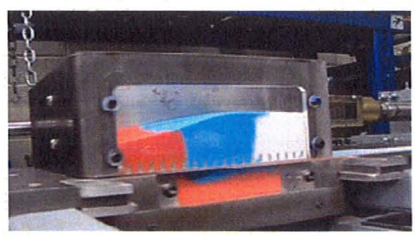

(g) 2.8 s

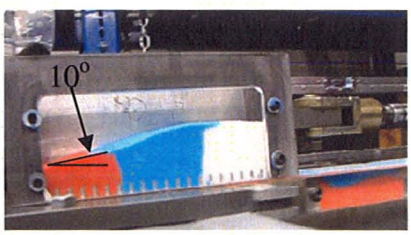

(h) 3.6 s

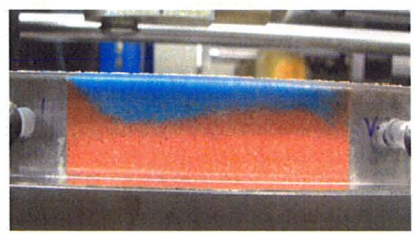

(i) 3.6 s

Figure 4.7. Powder flow pattern with TCCS bed at shoe velocity of (I) 170 mm/s and (II) 385 mm/s, using SPP1.

4.3. Influence of Increased Powder Level in the Shoe on Flow Patterns

In this section, the effect of powder level in the shoe on the flow patterns observed during filling is described. The extra weight is introduced in the shoe by (i) adding an extra layer of powder over the Tri-layer bed and (ii) by placing a hopper filled with powder over the front of the shoe to continuously feed the moving shoe with powder.

4.3.1. Die Filling using SS with Hopper

Fig. 4.8 shows the snapshots of the flow behavior of powder during die filling at a shoe velocity of 385 mm/s. The mass of powder on the front portion of the shoe is more than the rest of the shoe (Fig. 4.8a). It can be seen that the mass of powder placed in the hopper, exerts more pressure on the front stream of powder as the shoe translates over the die-cavity. As a result, the top layer (coloured in blue) flows with more intensity and fills three-fourth portion of the die (Fig. 4.8f). The difference in the packing pressure in front and rear side of the shoe makes the front stream deposit more powder into the die than the rest of the shoe (Fig. 4.8e). Further, as the shoe moves partially over the die, the white layer start to flow due to the force from the hopper powder mass (Fig. 4.8b). The white layer deposits small amount of powder near the top region, towards the right-side of the die as shown in Fig. 4.8c. In this case, nose flow dominates as no filling is contributed from the bottom layer in the case of standard shoe. The addition of the powder mass from the hopper has completely eliminated the formation of large gap in front portion of the shoe.

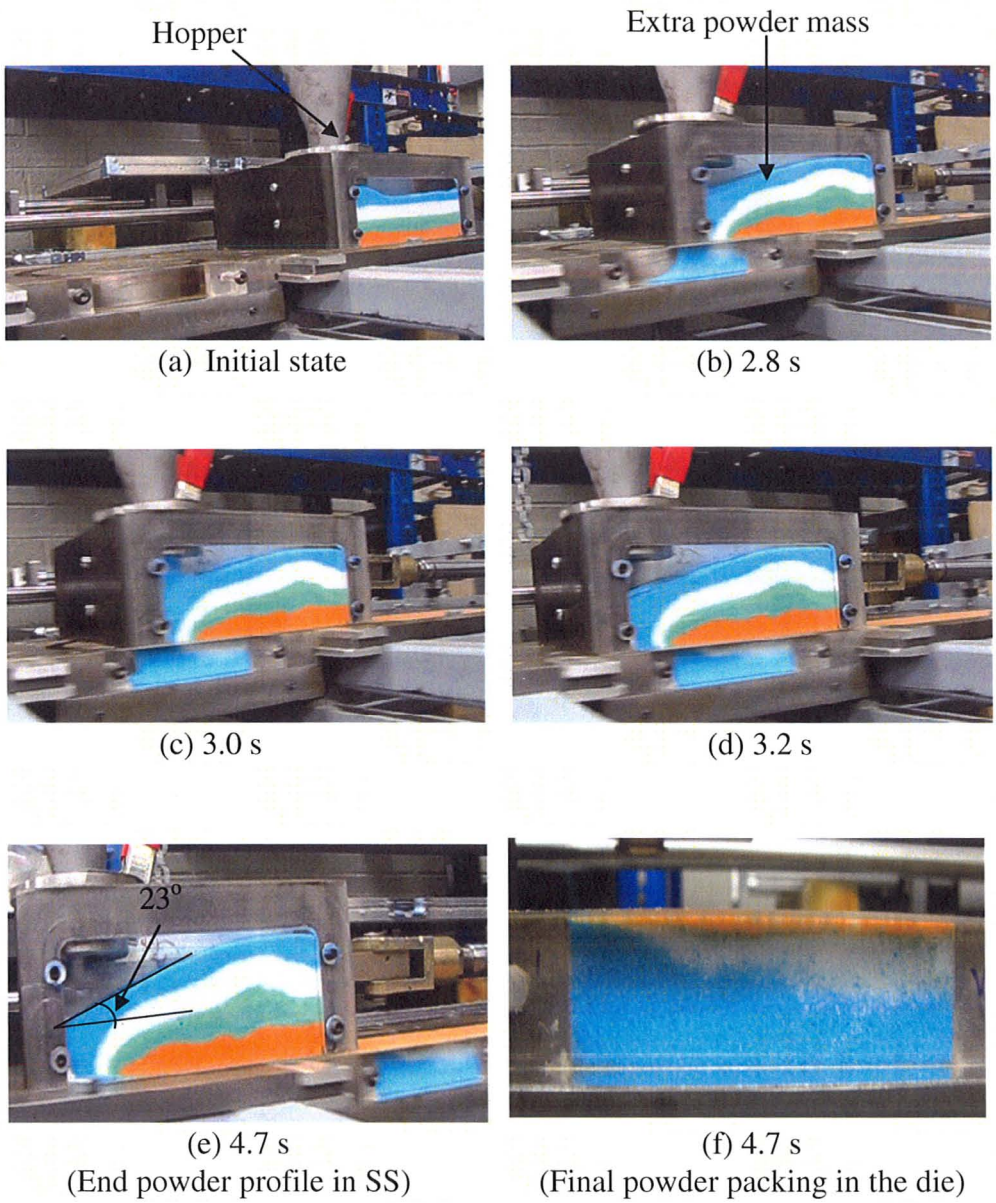

(a) Initial state (b) 2.8 s

(c) 3.0 s (d) 3.2 s

(e) 4.7 s
(End powder profile in SS)

(f) 4.7 s
(Final powder packing in the die)

Figure 4.8. Powder flow behavior during die filling with an increased powder mass in the shoe (SS) (V_{shoe}= 385 mm/s).

The end powder profile inside the shoe shows a post-avalanche angle of 23° in the front stream, which explains the rapid flow of powder vertically downward from the top

two layers. This means the powder from the hopper gets empty during the shoe motion using SS. Therefore, a slope in the powder bed is obtained in the front of the shoe. During the die filling using SS with standard powder level, all the three layer flows into the die-cavity. However, in the case of initially increased powder level and with the hopper delivering additional powder only top two layers take part in the filling.

4.3.2. Die filling using SPP1 with hopper

Results for SPP1 using hopper at a shoe velocity of 385 mm/s are shown in Fig. 4.9. As the shoe translates, the powder inside the hopper (particles coloured in black) drops in the shoe and compresses the powder layers in front of the shoe in the downward direction. Thus, powder from a front portion of the bottom layer inside the shoe is forced into the die-cavity. As a result, more particles from the bottom layer separate quickly and deposit into the die-cavity (Fig. 4.9d). As the shoe traverses further, and comes half over the die, white layer particles enter through the empty holes and fill the left-side of the die-cavity. Consequently, the mass of the white layer forces more powder from the bottom layer to enter the die (Fig. 4.9c). Thus, bigger portion of the bottom layer (i.e., from the leading edge to the center of the shoe) contributes to the filling process (Fig. 4.9d). Also to be noted is the pressure applied from the topmost layer and powder mass in the hopper on the leading side of the shoe. This pressure causes a depression in the powder layers, in the front portion of the shoe (Fig. 4.9 e). Further, segregation of powder into the die from all the three layers occurs during die filling with standard powder level (with three layers), whereas, in the case of powder deposition from a shoe with an increased level of powder material, only bottom two layers contribute to the filling. The post-avalanche

angle is not significant here, as steps are formed in different layers during the shoe motion.

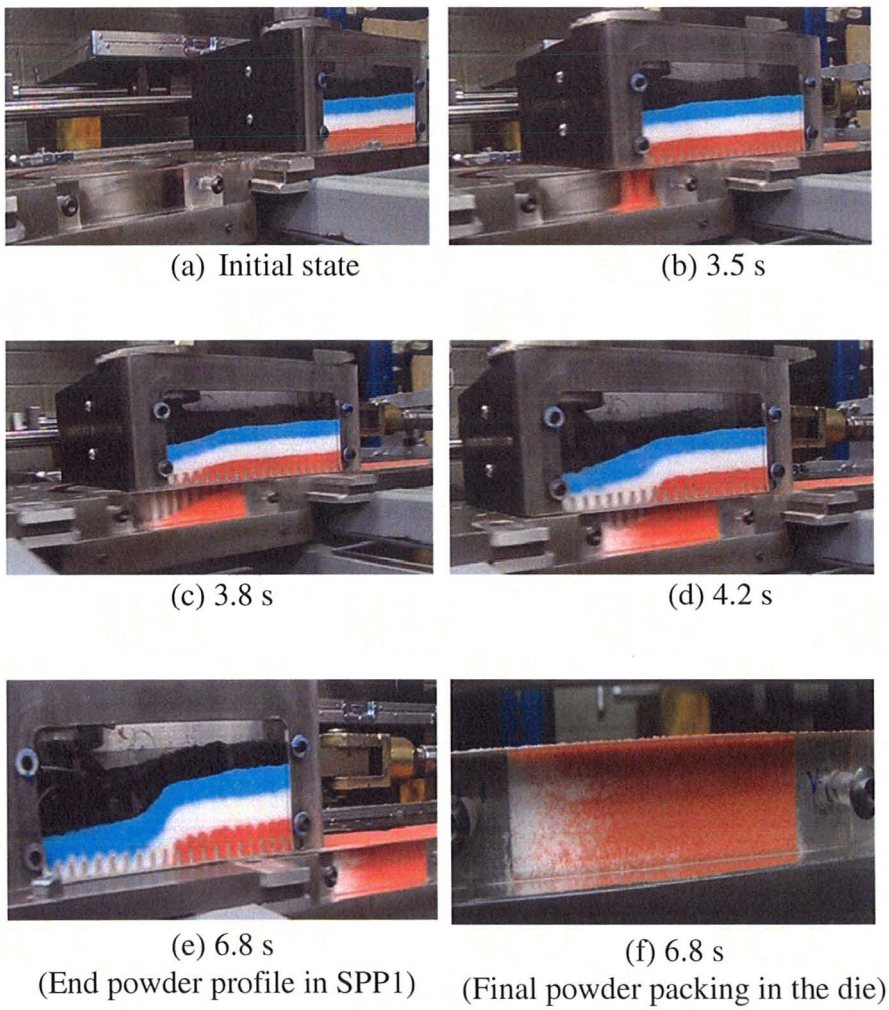

(a) Initial state (b) 3.5 s

(c) 3.8 s (d) 4.2 s

(e) 6.8 s
(End powder profile in SPP1)

(f) 6.8 s
(Final powder packing in the die)

Figure 4.9. Powder flow patterns at different times during shoe motion, using SPP1 (V_{shoe} = 385 mm/s).

4.4. Coloured iron powder flow analysis

Previous sections 4.1-4.3 presented results from coloured salt powder. In this section, die filling with coloured Fe powder was considered to explore the flow behavior of typically used fine metallic powder for P/M parts. This study also aims at comparing the flow patterns from coloured salt powder with the iron powder. The set-up of the coloured iron powder in three layers inside a feed shoe was similar to the earlier tri-layer coloured salt powder bed.

Fig. 4.10 shows the powder profile in the shoe and final particle packing inside the die-cavity at the end of the filling process using SS. It can be seen that, at a shoe velocity of 170 mm/s, a slope (post-avalanche angle) of 35^{o} is formed in the front stream of the powder. As a result, the top layer particles slide down rapidly into the cavity, and the rest of the powder mass moves towards the back of the shoe-wall with slight rearrangement of particles (Fig. 4.10b). Fig. 4.10c shows the end profile of the powder in the shoe after filling at a shoe velocity of 385 mm/s, a large space between the shoe wall, and the front stream of powder is created; this leads to the variation in the head packing pressure through the powder mass over the front and rear of the die-cavity. Therefore, density distribution inside the die-cavity gets nonuniform. A post-avalanche angle of 32^{o} is obtained in the powder bed in the shoe which is slightly smaller than the angle obtained at a shoe velocity of 170 mm/s, using SS. This means iron powder slope in SS also varies with the shoe velocity, like salt powder. The results obtained are similar to the coloured salt powder filling. It can be noted that the amount of powder poured inside the die, and the particle packing towards the back of the shoe may differ, due to the difference in the

particle density and the cohesiveness. However, the sequence of segregation of powder mass during filling with iron is similar to that observed in salt filling.

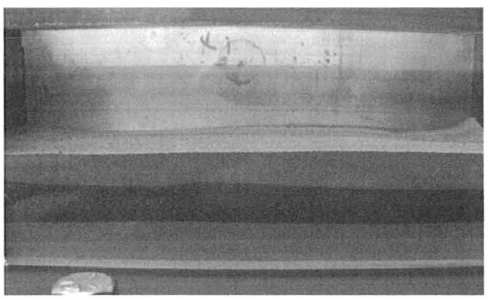

(a) Initial state

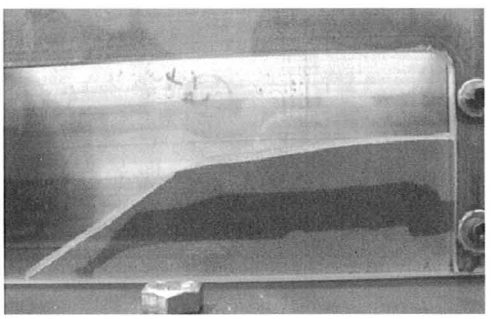

(b) At shoe velocity of 170 mm/s

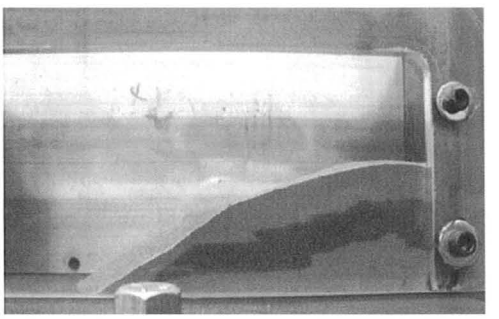

(c) At shoe velocity of 385 mm/s

Figure 4.10. Powder profiles in the feed shoe after the first pass of die filling using SS.

During die filling using SPP1 with iron powder at a shoe velocity of 170 mm/s (Fig. 4.11), the particles in the bottom layer detach from the powder mass through the holes of the perforated plate and drop first in the die-cavity. The powder profile inside the shoe shows some packing towards the back of the shoe and a stepped profile in the front. It is also observed that the top layer is pushing the middle layer, which creates a step profile in the front of the shoe. Further, the top layer also

flows in small amounts inside the die. However, at 385 mm/s, the powder profile in the shoe shows that the complete bottom layer flows into the die-cavity (Fig. 4.11c). As a result, the major particle deposition occurs from the bottom layer.

The results obtained in the case iron powder are different from the coloured salt when a filter is used to deliver the powder. During salt mixture filling at 385 mm/s, all the three layers were flowing inside the die-cavity through the front portion holes (Fig. 4.4), whereas for the iron powder filling the entire bottom layer passes through the holes and few particles from the middle layer also flow into the die. In addition, for the iron powder, the powder profile in the shoe showed a small post-avalanche angle of 5^{o} near the front, and the rest of the layers were intact.

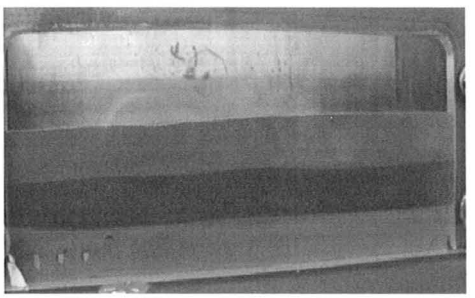

(a) Initial state

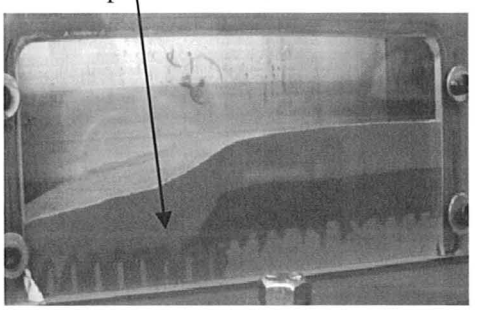

(b) At shoe velocity of 170 mm/s

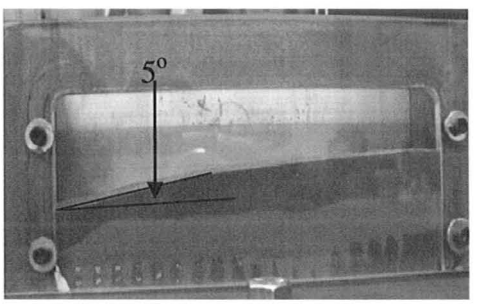

(c) At shoe velocity of 385 mm/s

Figure 4.11. Powder profiles in the shoe and the die-cavity after die filling with SPP1.

This part of the results explains the similarity between the flow behavior of the tri-layered salt powder and tri-layered iron powder. Although, salt and iron powders have different particle size and physical properties, still salt flow in general mimics the iron powder flow on the macroscopic level. Thus, better visualization of coloured salt powder was a benefit to define the criticality of the flow behavior of the iron powder material during the filling process.

4.5. Influence of shoe velocity on powder filling rate in the die

Table 4.1 presents results of the filling rate as a function of shoe speed for SS and SPP1 shoe configuration. It is evident that there exists a maximum shoe velocity at which the die can be completely filled, which is referred to as critical shoe velocity (Wu et al., 2003c). As the shoe (SS) speed changes from 120 mm/s to 170 mm/s, filling rate increases by 53 g/s (i.e., from 93 g/s to 146 g/s). However, as the speed increases further, i.e., from 170 mm/s to 240mm/s and from 240 mm/s to 385 mm/s the filling rate shows a small increase of 17 g/s and 21 g/s respectively. Therefore, the critical shoe velocity for die filling with SS is 385 mm/s in the current die-fill system. It is also observed that, in the case of filling with SS, the die is completely filled in one pass till 385 mm/s. Further, at a shoe speed of 240 mm/s mass of powder filled inside the die reaches a maximum.

Table 4.1. Iron powder filling rates with SS and SPP1 for different shoe velocities.

Shoe speed, (mm/s)	Total mass, (g) SS	Total mass,(g) SPP1	Filling time (s)	Filling Rate, (g/s) SS	Filling Rate, (g/s) SPP1
120	232.3 ±0.57	253.3±0.57	2.5	93	101.32
170	234	234.3±0.57	1.6	146.18	146.4
240	254.3±0.57	210.6±1.52	1.56	163.14	135
385	248.5±1.2	173.3±0.57	1.35	184.07	128.4

For SPP1, Table 4.1 shows that the powder filling rate increases as the shoe velocity increases, until it reaches maximum, thereafter average filling rate decreases with the increasing shoe velocity. At a shoe velocity of 170 mm/s, the die is completely filled in a single pass, during filling from SPP1, whereas, above 170 mm/s, more than one pass is required to fill the die-cavity completely. Thus, the critical shoe velocity for die filling with SPP1 is 170 mm/s, which is much lower than the critical shoe speed for die filling with SS. At higher shoe velocities with SPP1, the trailing side (right-side of the die-cavity) remains partially filled, as the powder passes very slowly through the holes in the rear side of the shoe and the front stream quickly moves over the die. Clearly the amount of powder that passes through the holes is a function of hole-diameter and hole-spacing.

Table 4.2 presents the results of powder filling rate into the die using a shoe with hopper. Again, both SS and SPP1 cases were considered. Average mass flow rate of the

powder is somewhat higher than that obtained for standard powder level (i.e., without hopper) at different shoe velocities. However, there is no significant change in the filling rate at different shoe velocities for SPP1 filling. In this case, bottom layer delivers more powder than the top layers in the die. Since, powder interlocking at the bottom increases by the increasing the powder level inside the shoe, the particles face difficulty in flowing through the holes into the die. As a result, no significant increase in the filling rate is observed in SPP1 with the addition of hopper. However, the hopper on the front of the standard shoe forces powder to flow more intensely into the die (nose flow).

Table 4.2. Iron powder filling rates with hopper at different shoe velocities.

Shoe speed, (mm/s)	Total Mass,(g) SS	Total mass,(g) SPP1	Filling time (s)	Filling Rate, (g/s) SS	Filling Rate, (g/s) SPP1
120	263.3 $\pm$1.15	250	2.5	105.4	100
170	259	231.3$\pm$0.57	1.6	161.8	144.6
240	258.2$\pm$1.73	197.6$\pm$3.78	1.56	165.4	126.7
385	252	175.6$\pm$1.15	1.35	186.6	130.1

4.6 ARAMIS results

4.6.1. Qualitative observations

Camera images of the die filling process were recorded using a high-speed camera with a close view of the die-cavity. In this section, some interesting features of iron powder segregation from SS and SPP1 at a shoe velocity of 170 mm/s are presented. The powder flows into the die-cavity with a mass flow from a SS (Fig. 4.12). The flow of the powder is observed from two directions; in the direction of the shoe motion and perpendicular to the direction of shoe motion (i.e., over the die-core) as shown in Fig. 4.12b. The stream of larger particles with higher velocity moves ahead as the shoe traverses, whereas the smaller particles settle down and rearrange near the bottom of the avalanche. Thus, size induced segregation takes place.

In SPP1, the powder flowing through the holes is dropping straight in the die-cavity. The standpipe flow is forming a stepped profile inside the die, which is similar to the avalanche stratification of powder (Fig. 4.13a). The avalanche stratification occurs due to size and shape induced segregation, which makes fine particles remain at the top and coarser particles cascade down near the bottom of the avalanche. Further, the entrapped air in the powder mass can also be seen in the rear perforated plate holes, which indicates that the air escapes out from the die by percolating through the holes (Fig. 4.13). The intermittent flow through the rear holes is due to the effect of air flow. This indicates that the effective area through which the material flows is smaller; thus, the mass flow rate is reduced. It is also noted that the top right corner of the cavity is filled at the end during forward stroke of the filling process.

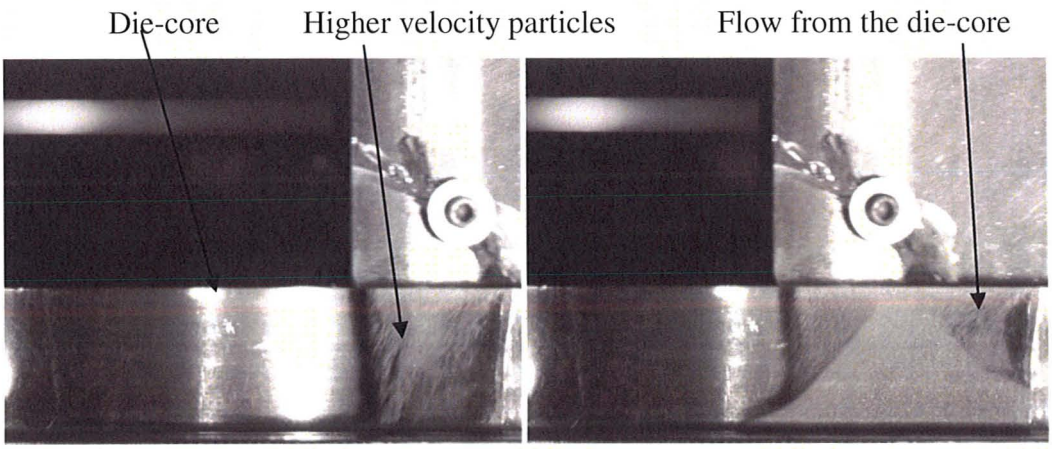

(a) 0.5 s (b) 0.55 s

Figure 4.12. Snapshots of powder flow from SS during filling process.

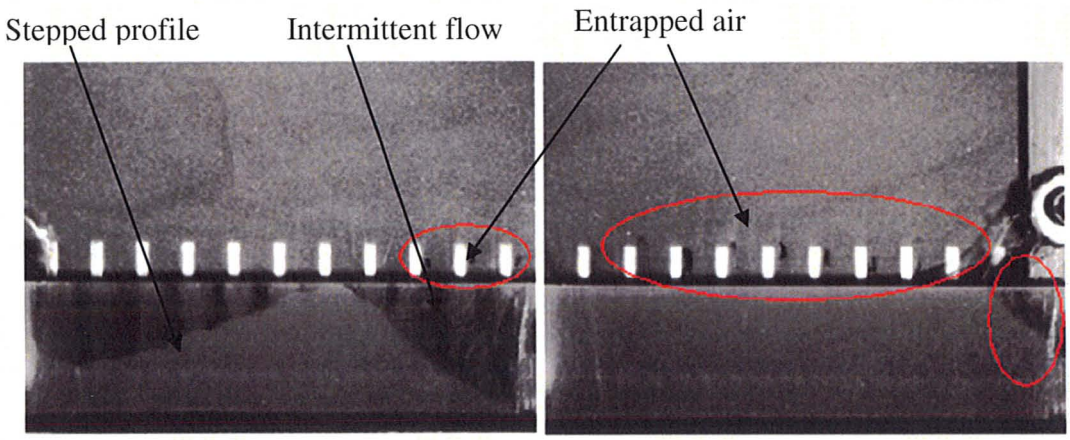

(a) 0.8 s (b) 1.40 s

Figure 4.13. Snapshots of powder flow from SPP1 during filling process.

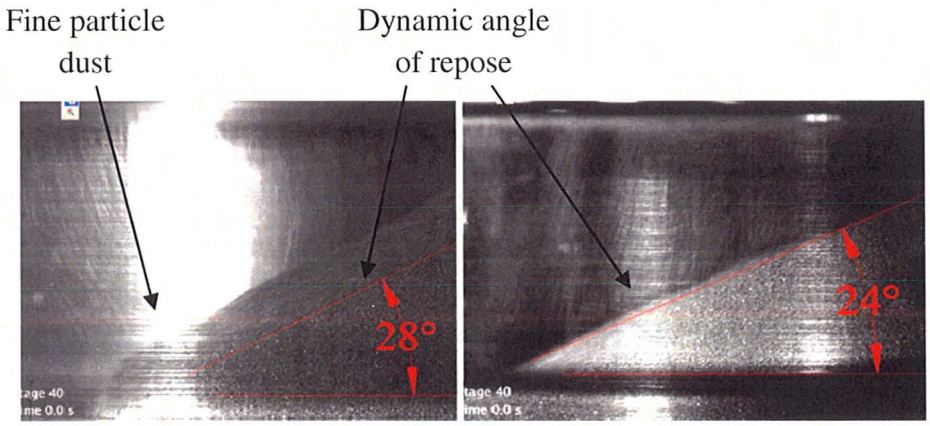

Figure 4.14. Avalanche behavior of powder in the die, using (a) SS and (b) SPP1.

Figs. 4.14a and b show the avalanche behavior of the powder flowing through SS and SPP1 respectively. The dynamic angle of repose for iron powder from a SS and SPP1 filling are 28^{o} and 24^{o} respectively, which is higher than the static angle of repose calculated for the same powder, i.e., $20\text{-}23^{o}$, (Section 3.7.2, Chapter 3). This confirms that the flow behavior of powder in static and dynamic modes is different. In addition, the dynamic angle of repose in SS filling is slightly higher than the SPP1 filling which is due to more uniform and controlled flow from the perforated plate. The flow from SS shows lot of fine particle dust over the avalanche due to turbulent flow of powder during filling whereas the flow through SPP1 is less turbulent and shows negligible fine dust cloud over the avalanche.

4.6.2. Displacement contours along X-axis

In this section, the data with regard to displacement of the particles tracked along X-axis during forward and retraction stroke of the filling cycle is presented. ARAMIS presents the results in the form of spatial displacement maps, where each colour represents a different displacement level.

Fig. 4.15 shows the displacement of particles at two points A and B in the die, when the SS is traversing over the die-cavity. The shoe is moving from right to left. The different contours correspond to different relative displacements. In this calculation, points A and B are located at the top right and the bottom of the die-cavity respectively. When the shoe is over the die-cavity in the forward stroke both points (in red shaded area) show small displacement in the right-side of the die (Fig. 4.15a). However, the smaller portion at the top shaded in blue represents larger displacement in the forward direction. As the shoe moves across the die in the forward direction, points A and B show slight movement in the forward direction whereas in the top particles show significant movement in the trailing side of the die-cavity (Fig. 4.15b and c).

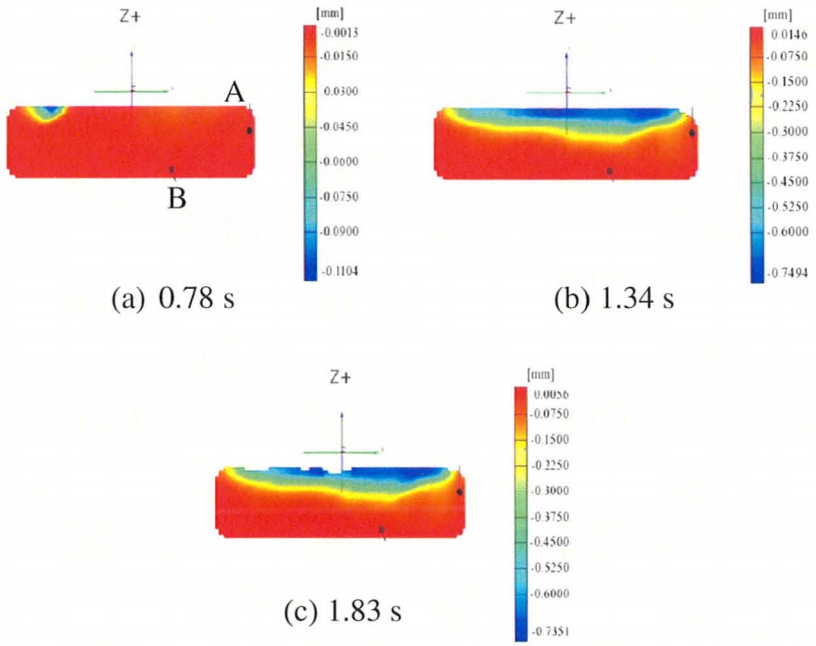

Figure 4.15. Displacement contour of powder in X-direction during forward stroke using SS (V_{shoe}= 170mm/s).

In Fig. 4.16, the displacement of point A and B in the die during the retraction stroke of the shoe is presented. As the shoe starts to move backward, both points show small displacement towards the trailing side of the die. In the top region of the die-cavity particles show significant movement in the leading side (Fig. 4.16a). However, when the shoe translates over the die-cavity, A and B points show insignificant movement in the leading side of the die, but the small portion in the top shows substantial displacement of particles towards trailing side (Fig. 4.16b and c)

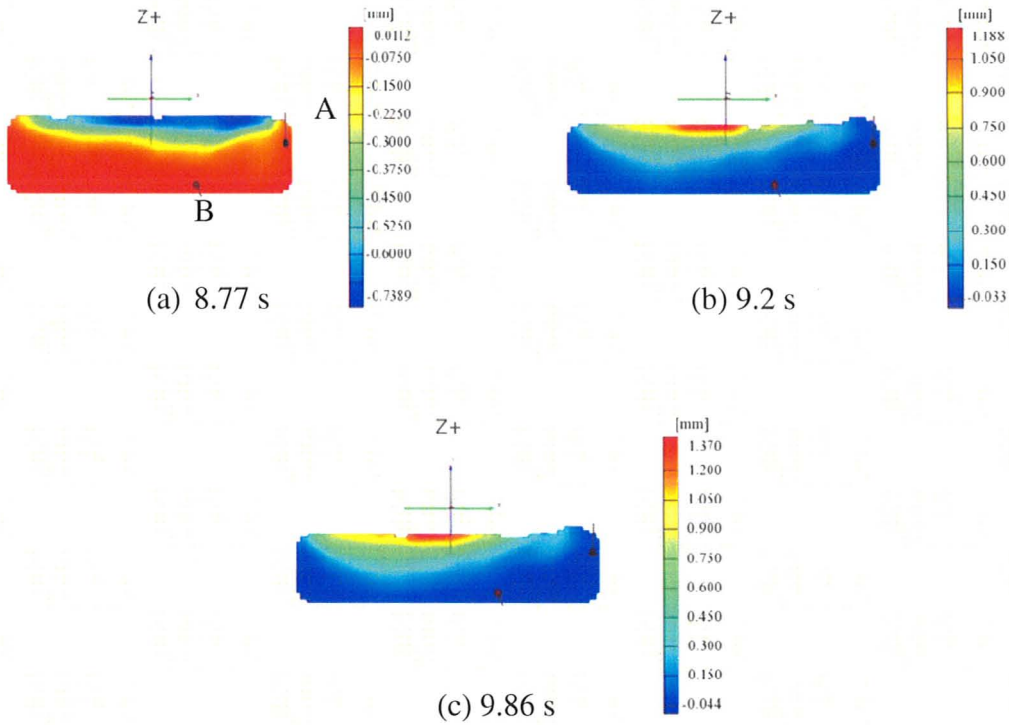

Figure 4.16.Displacement contour of powder in X-direction during retraction stroke, using SS (V_{shoe}= 170mm/s).

In SPP1, during the forward stroke, particles at points A and B in the die show insignificant displacement towards the right-side (trailing side) of the cavity (Fig. 4.17a). As the shoe moves further, both particles reveal negligible movement, but at the end of the forward stroke, minor movement of points A and B is noted. However, at the start of the retraction stroke (Fig. 4.18), point A shows minor displacement towards the leading side and point B moves slightly towards the trailing side of the die (Fig. 4.18a). For the rest of the stages, during retraction of the shoe, points A and B show relatively small displacement towards the trailing side of the die-cavity (Fig. 4.18b and c). Top region

shows significant movement during the retraction of the shoe, which means additional powder is flowing into the die-cavity.

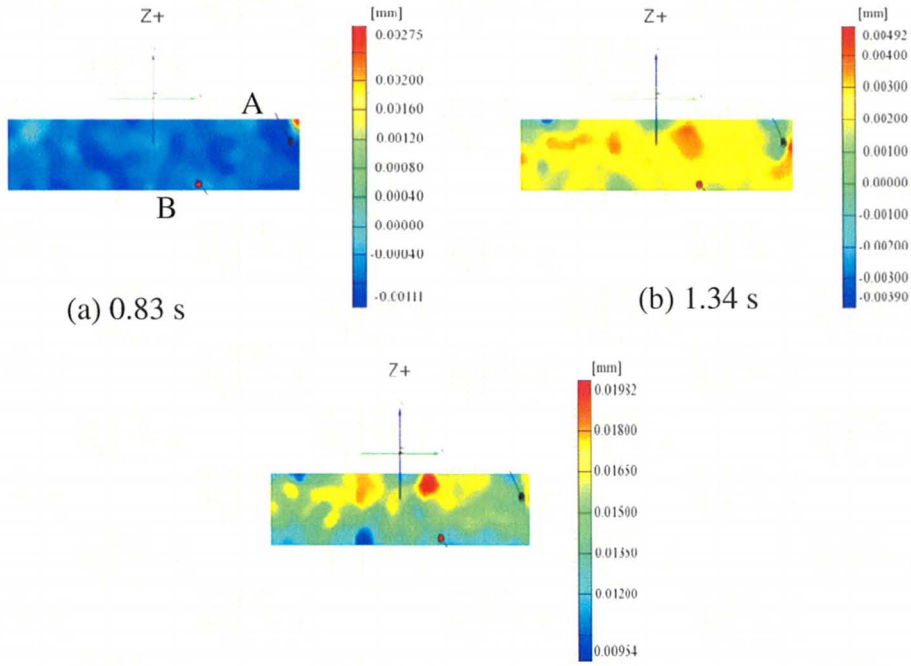

Figure 4.17. Displacement contour of powder in X-direction during forward stroke, using SPP1 (V_{shoe}= 170mm/s).

Overall, displacement of particles along X-axis in the case of SPP1 filling is significantly smaller than the displacement for the case of SS. The results are consistent with the earlier filling rate data (Table 4.1).

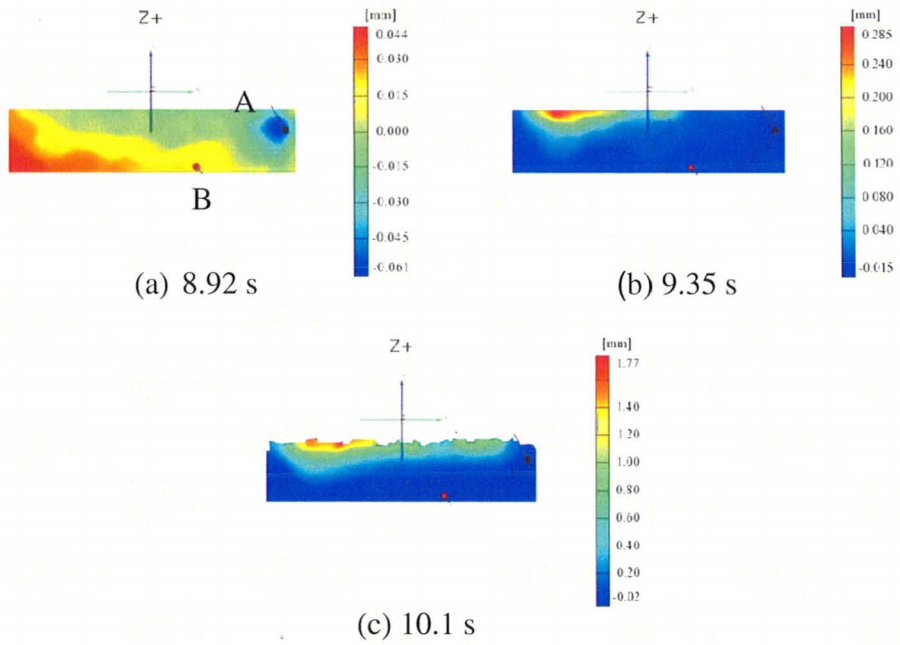

Figure 4.18. Displacement contour of powder in X-direction during retraction stroke, using SPP1 (V_{shoe}= 170mm/s).

4.6.3. Displacement contours along Y-axis

The Y-displacement of powder during forward and retraction stroke of the filling process were studied to understand the vertical segregation of the powder.

With a standard shoe moving at a velocity of 170 mm/s, the movement of the particles at points A and B during the forward stroke of the filling process is shown in Fig. 4.19. The shoe is moving from right to left, and the position of points inside the die is similar to the previous case. It can be seen that points A and B, show minute displacement in the downward direction when the shoe is entirely over the die (Fig. 4.19a).

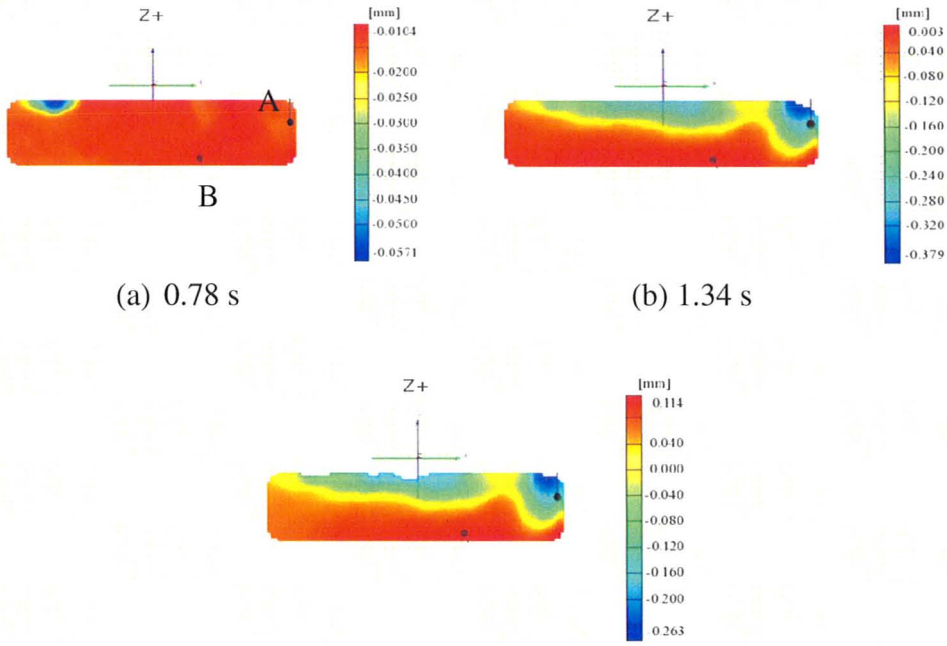

(a) 0.78 s (b) 1.34 s

(c) 1.83 s

Figure 4.19. Displacement contour of powder in Y-direction during forward stroke, using SS (V_{shoe}= 170mm/s).

As the SS moves further, point A shows a considerable amount of displacement in the downward direction in the die-cavity, whereas point B represents a small displacement in the upward direction (Fig. 4.19b). The compressive forces acting from the shoe on the filled die pushes the particles downwards up to some distance from the top, and this movement pushes the bottom particle to create their own space. Thus, during the rearrangement particle moves slightly in the upward direction. At the end of the forward pass, the movement of point B (bottom region) becomes significant in the upward direction, whereas point A (top region) moves downwards substantially (Fig.

4.19c). Fig. 4.20 shows displacement map of the particles moving along Y-axis during the retraction stroke for SS. In this case, point A shows significant movement in the downward direction relative to point B. This indicates that additional powder is filled into the die during retraction stroke and some rearrangement of particles at the top occurs. Further, towards the end of the retraction stroke, both points A and B move in the downward direction. However, point B moves a smaller amount than point A.

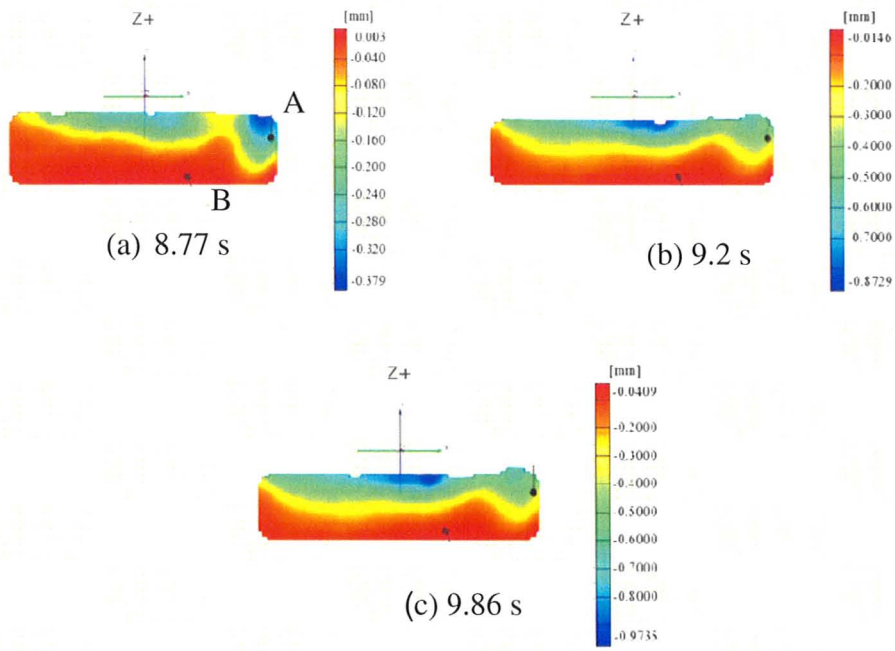

Figure 4.20. Displacement contour of powder in Y-direction during retraction stroke, using SS (V_{shoe}= 170mm/s).

In SPP1 filling, particle displacement along the vertical axis is found to be negligible as compared to the displacement in SS filling. Both points in the die cavity during the forward stroke at different times of the shoe motion show insignificant displacement in Y direction (Fig.4.21). However, during the initial stage of retraction

stroke, points A and B show small upward movement, and in the intermediate stages particles show stagnant behavior (Fig. 4.22a and b). At the end of the retraction stroke, points A and B show relatively larger displacement in the upward direction (Fig. 4.22c).

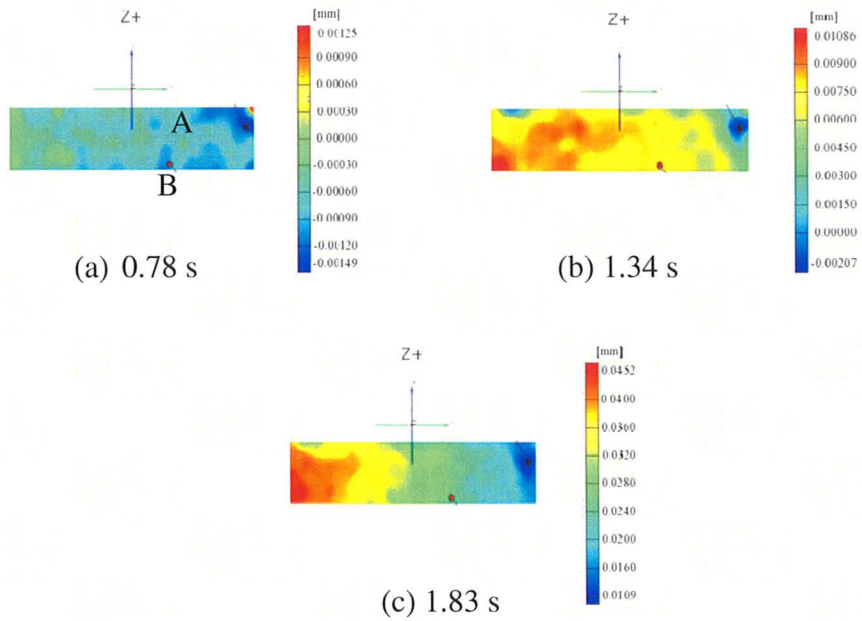

Figure 4.21. Displacement contour of powder in Y-direction during forward stroke, using SPP1 (V_{shoe}= 170mm/s).

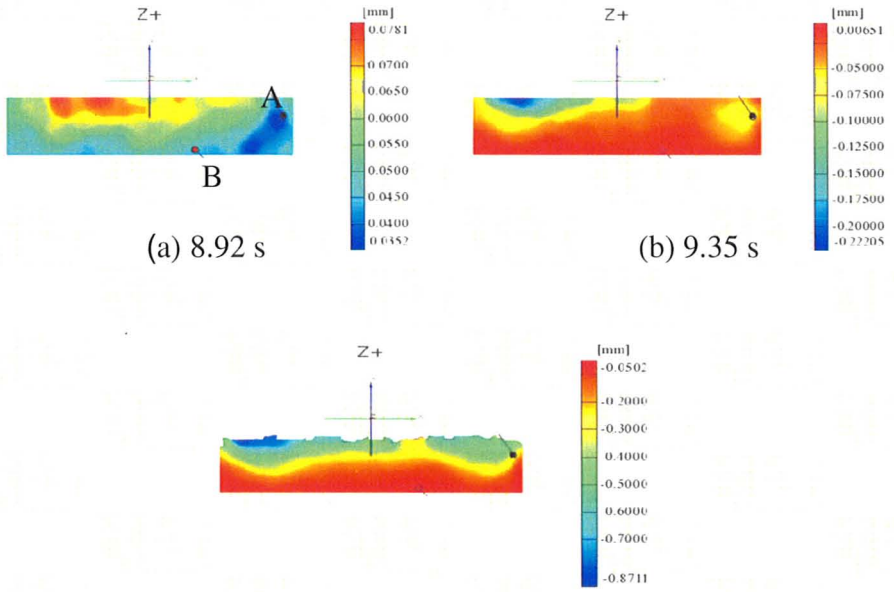

Figure 4.22. Displacement contour of powder in Y-direction during retraction stroke, using SPP1 (V_{shoe}= 170mm/s).

Figs. 4.23 and 4.24 present a comparison between SS and SPP1 for the horizontal and vertical displacements at the earlier 2 locations (points A and B) within the die as a function of time. It is clear that the rearrangement of top and bottom region is significantly different with SS filling during the forward stroke in both X and Y directions; thus, the packing density also varies in both regions. However, in the case of SPP1, displacement maps show that the top and bottom particles are rearranging uniformly along x-axis and both points (A and B) show comparatively small displacement than in SS filling. Along Y-axis, it is observed that in SPP1 points A and B are showing small displacement in forward stroke, but in retraction stroke, point B displaces more than A. However, both points in SS show higher displacement than in

SPP1. In addition, the mass added to the die top region, and the packing pressure varies significantly in the SS during the retraction stroke. However, the perforated plate holds same quantity of powder in all the holes over the top region of the die-cavity, which applies equal pressure on the front and rear of the die-cavity top. This leads to a uniform packing of the powder in the die during SPP1 filling.

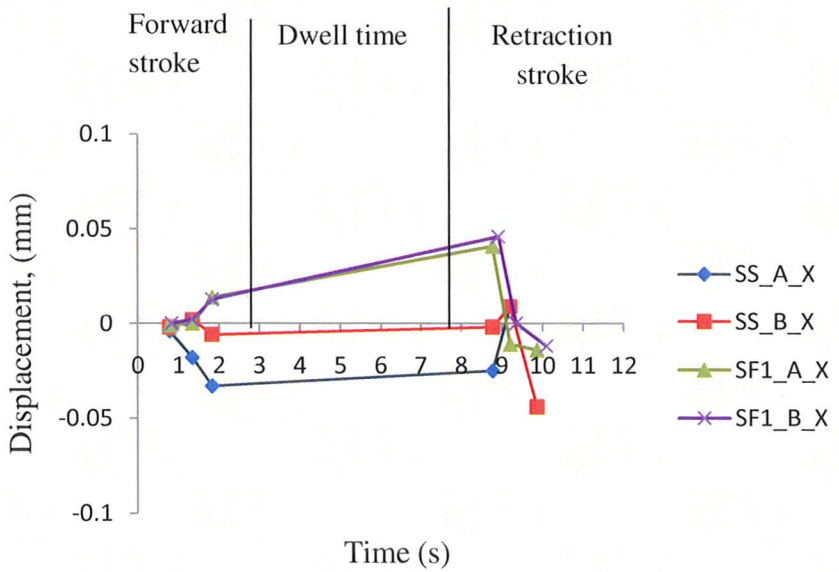

Figure 4.23. Comparison of SS and SPP1 displacement traces at two locations (A and B) in the horizontal direction as a function of time.

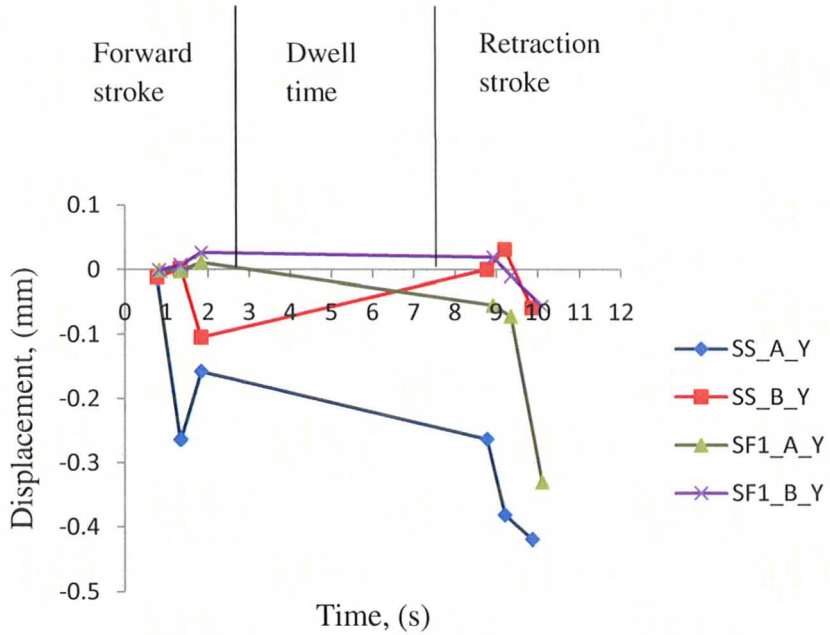

Figure 4.24. Comparison of SS and SPP1 displacement traces at two locations (A and B) in the vertical direction as a function of time.

4.7. Surface porosity measurement by Image Analyzer

The percentage porosity measurement on the transparent die face (TDF) was conducted after complete die filling process to study the uniformity of iron powder particle distribution for die filling methods with SS, and SPP1. In order to measure the repeatability of porosity distribution 8 filling tests for SS and SPP1 techniques were conducted. The data was analyzed for six point locations on the TDF as shown in Fig. 4.25 (cross-refer to Fig. 3.15 of Chapter 3).

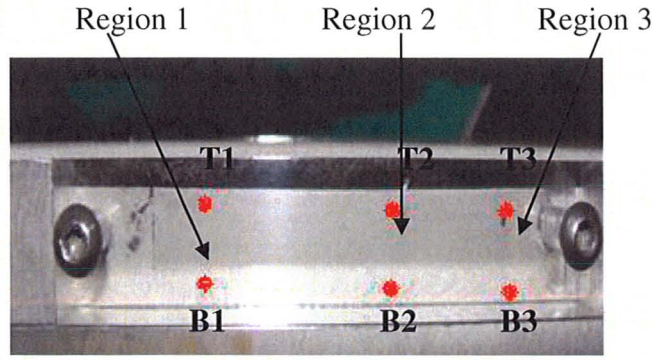

Figure 4.25. View of different point locations on the transparent die-cavity face for porosity measurement.

In all results reported here, Points T1, T2, T3, B1, B2, and B3 in the die-cavity were fixed for all the tests. This study was conducted with a shoe velocity of 170 mm/s. For die filling process performed using a SS, results indicate difference in porosity distribution in the top and bottom regions of the die surface (Fig. 4.26). The top locations exhibit a higher porosity at T1 and T3 locations compared to B1 and B3 locations, whereas T2 shows slightly less porosity than B2. An overall porosity data on the die surface in the region 1, 2, and 3 for SS filling shows nonuniform distribution. Similar results for SPP1 indicate a more uniform porosity throughout the TDF (Fig. 4.27).

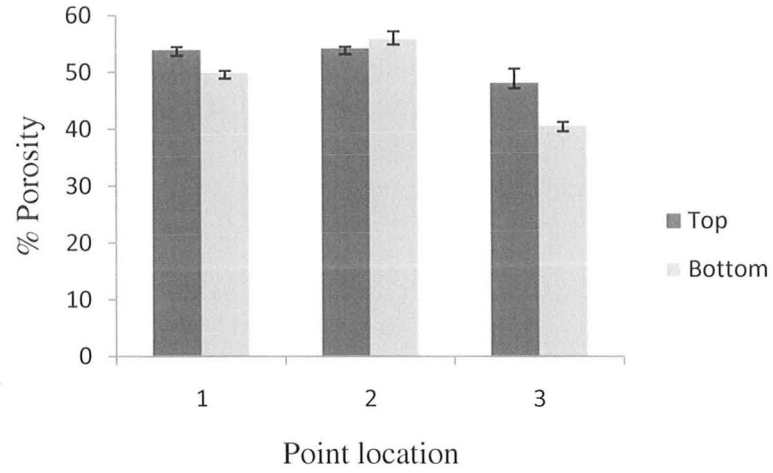

Figure 4.26. Percentage porosity difference between top and bottom surfaces on TDF, using SS.

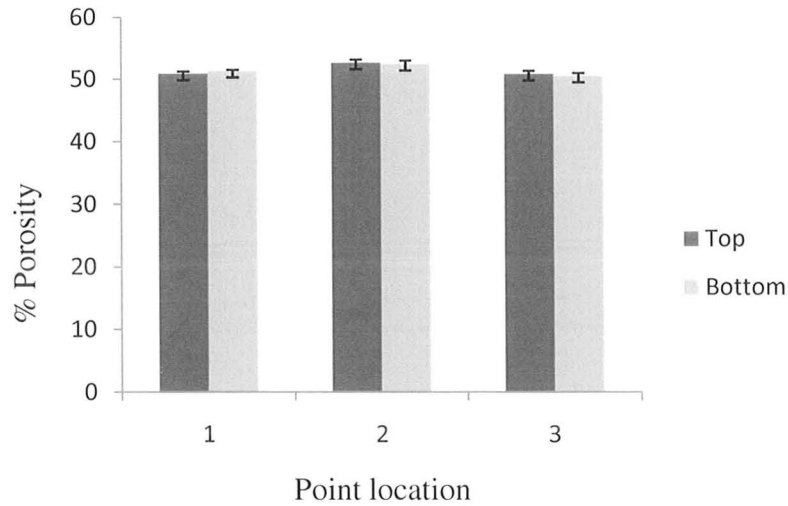

Figure 4.27. Plot of percentage porosity in top and bottom locations on TDF, using SPP1.

By comparing SS and SPP1 porosity data, it can be seen that the percentage surface porosity for T1, B2 and T2 point locations is decreased with the use of SPP1, whereas surface porosity at T3, B3, and B1 location is increased substantially. Therefore, the results indicate that there is no significant overall reduction in the magnitude of porosity with the use of perforated plate-1.

The results of surface porosity data can be compared with the earlier ARAMIS displacement maps of the particles during forward stroke and the reverse stroke of SS and SPP1 filling process (Section 4.6). It is clear that top region particles rearrange during the forward stroke, even after the die is filled, when the filling is performed using SS. This is due to the interaction of the particles at the top of the die-cavity with the particles at the bottom of the shoe. Thus, variation in the porosity of the top and bottom region occurs. In the case of filling using SPP1, as mentioned in the previous section, the rearrangement of the powder takes place simultaneously in the top and bottom region of the die-cavity surface as the shoe moves over the die-cavity (Fig. 4.21 and Fig. 4.22). Therefore, the powder packing is more uniform in the case of SPP1 filling.

4.8. Gamma ray densitometry results

Powder sintering technique was applied to the die in the filling state using iron powder mixture and SS and SPP1 gravity filling methods at a speed of 170 mm/s. The shape of the die filled powder after sintering is shown in Fig. 4.28. The ring-shaped sample was divided in two symmetric halves (left and right sides). Three equal-sized

rectangular parallelepiped pieces were sectioned from each side and weighed on the laboratory weight scale.

A sample size of 14 mm x 12 mm x 10 mm was cut from each section to determine the void fraction within the sample using gamma densitometry. The transmitted gamma rays were counted by using multichannel analyzer in pulse height analysis mode. The pulse count for the background without placing the source was recorded as N_b= 255 (Fig. 4.29a). The attenuated fluxes count for the empty system, N_{Cg}=1, for a dense sample, N_{Cg}=0, as well as for the actual sample, N_{Cg} was obtained from the multichannel analyzer. Full energy peak shown in Fig. 4.28b corresponds to unscattered gamma rays. The small energy peak in Fig. 4.29c indicates that the gamma rays are absorbed to a large extent by the dense reference sample. The attenuation count measurement for each section was repeated three times to get accurate reading.

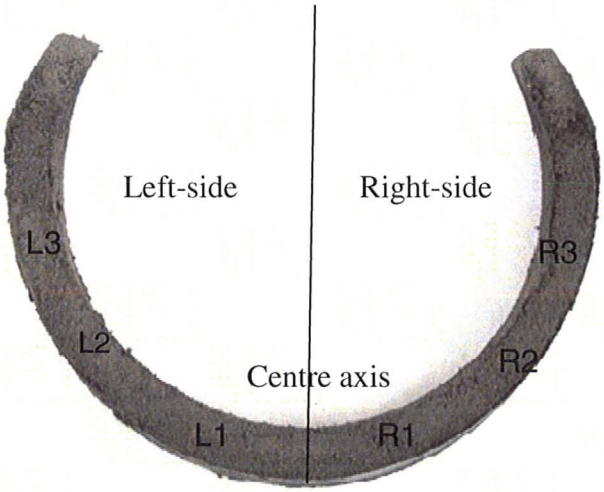

Figure 4.28. Location of six sections on a resin-bonded sample for density analysis.

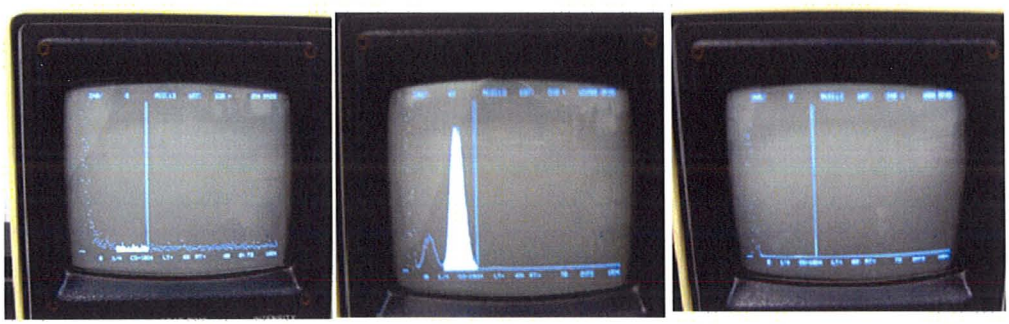

(a) (b) (c)

Figure 4.29. Attenuated fluxes count for a) background, b) empty, $N_{\epsilon g}=1$, and c) with dense reference sample, $N_{\epsilon g}=0$.

The void fraction calculation was done by using the formula mentioned in Section 3.8.2. The count rate of the background was subtracted from all the count rates obtained. The % voids in different section of the heated sample obtained by using Gamma densitometer are illustrated in Table 4.3. The average void percentage in the left region is 8% higher than in the right region for SS filled sample. However, in the case of the bonded sample from SPP1 filling, the average void percentage in the left region is only 0.6% higher than in the right region. The void distribution in the sections L1 and R1 which are closer to the central axis (sections parallel to the shoe motion) are more uniform in SPP1 sample than in SS. However, void distribution is slightly uneven and higher in the sections L2, L3, R2, and R3 (perpendicular to the shoe motion) in SPP1 filled samples. In the case of SS, the distribution is throughout nonunifrom in the die.

The results from the surface porosity measurement which are taken in the front region (i.e., in the sections parallel to the shoe motion) for SPP1 are consistent with the bulk porosity measurement in those sections for SPP1 (Fig. 4.27).

Table 4.3. Void percentage in different sections of the heated sample.

Sections	% Voids	
	SS	SPP1 filling
L1	36.05	34.56
L2	34.2	39.7
L3	31.6	39.4
Avg.	35.28	37.86
R1	31.05	33.02
R2	32.7	40.6
R3	33.6	39.26
Avg.	32.45	37.63

4.9. General features of powder flow from SPP2

A perforated plate is with slant holes at an angle of 15° and orient in the backward direction towards the rear of the shoe PP-2, was tested to understand the effect on the flow behavior of powder from the perforated plate holes at some significant angle. The flow of powder from SPP2 was also recorded with the high-speed video system (Figs. 4.30a and b). During the initial stages of filling using PP2, the particles flow at an angle through the holes with the direction of the flow opposite to that of the hole-orientation. The orientation of the hole-angle selected for this plate made the flow of powder difficult; thus, uncontrolled flow is observed. Also, in the right corner of the die-cavity the powder drops straight from the die-core and fills the cavity in the direction perpendicular to the

shoe motion (Fig. 4.30a).

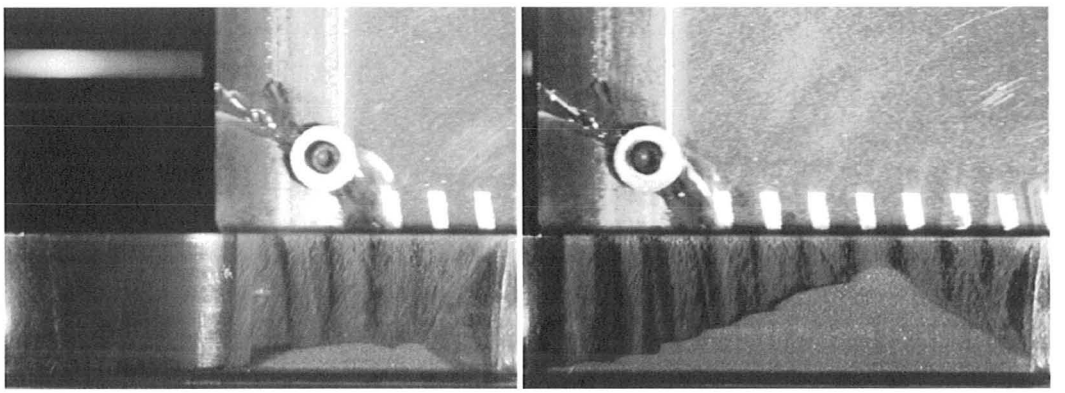

(a) (b)

Figure 4.30. Snapshots of powder flow from SPP2 during filling process (iron powder).

To evaluate the porosity data distribution using SPP2, surface porosity analysis using image analyzer was performed. Fig. 4.31 shows that the porosity is significantly non-uniform in region 3 for SPP2.

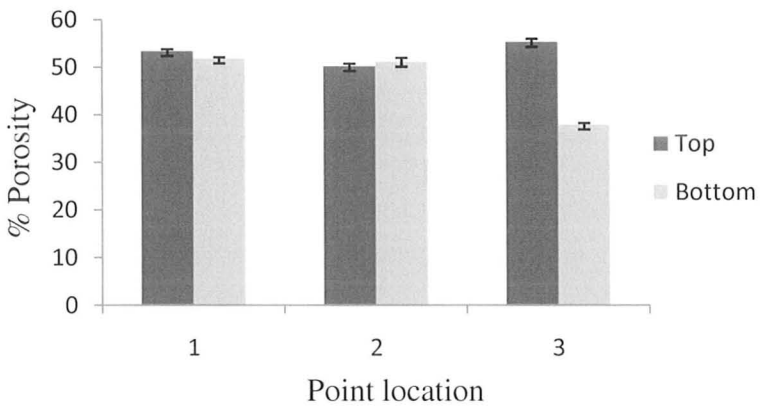

Figure 4.31. Percentage porosity difference between top and bottom regions of the die-cavity surface using SPP2.

Further, by comparing the average porosity data for SS and SPP2 filling, it is observed that surface porosity at T1 and B1 location is not changed even after using SPP2 filling method. However, in T2, B2, and B3 location percentage porosity is reduced with the use of SPP2 (Fig. 4.26). Only for T3 location the use of SPP2 has not shown any improvement in porosity reduction. From the surface porosity results, it is clear that the porosity data calculated at six specified locations for the die filling SPP1 shows remarkably uniform distribution, whereas for SPP2 has not improved the particle distribution in the die. This chapter presents only a few results from SPP2 filling. The experiments were largely unsatisfactory and did not point to any benefits with the backward orientation of the holes. More careful design of the hole-orientation will be needed to analyze the effect of orientation on the fill characteristics.

CHAPTER 5

DISCUSSION

5.1. Segregation during die filling

In this research, an attempt has been made to understand the macroscopic flow patterns of the powder during die filling process with the help of a laboratory-built die-shoe fill system. The coloured powder experiments worked well in depicting the types of flow, powder segregation during filling, and final particles packing in the die. For these experiments, it was made sure that a fine quality of salt is coloured uniformly without affecting its flow properties. It is found that the salt powder profiles in the shoe and sequence of segregation of layers and flow patterns closely mimic with the iron powder flow patterns (Section 4.2). The results confirm that the salt with its better colouring attributes and resulting images quality during the die filling experiments offers an efficient medium to demonstrate the macroscopic flow behavior of the iron powder under different test conditions. The coloured powder experiments were divided in two parts; with tri-layer mixture, and with tri-column mixture. The tri-column powder bed tests were performed to understand the effective area of powder delivery across the length of the shoe.

During the die filling in a ring-shaped die-cavity, at a shoe velocity of 170 mm/s, flow of powder in two directions was observed in the die. Near the die-cavity entrance, powder flows from the shoe translating over the die as well as vertically downward from the core of the die which pushed the powder in perpendicular direction (Fig. 4.12b).

As the standard shoe starts from rest the powder mass inside the shoe moves towards the back of the shoe-wall, which results in close packing of the particles in the rear portion of the shoe. As a result, a gap is created in front of the shoe, as shown in Fig. 4.2 and Fig. 4.3. The depression developed in the front powder mass affects the mass flow rate and the packing pressure uniformity. Firstly, creation of the gap means that powder is not delivered into the die across its full cross-section, which in turn explains that the mass flow rate is lower from the rear portion of the shoe. Secondly, the packing pressure applied by the powder mass in the shoe also varies on the left and right sides of the die-cavity. On the positive side, the gap created in the front of SS provides an easy channel for the air to escape; thus, increasing the filling rate in the first and reducing the entrapped air in the die-cavity.

It is noted that the free particles from the top surface of nose shaped profile falls into the die-cavity in the case of standard shoe (SS). At this stage, the air inside the die cavity tries to escape out of the die. The air makes an escape route from the trailing side of the die-cavity through the gap created in front of the shoe or percolates through the powder mass in the shoe. However, in the SPP1 case, very small gap is created in the front, and thus, air evacuates mostly through the powder mass inside the shoe (Fig. 4.13).

The fact that air flow interferes in the powder free flow is consistent with the flow examined through SS and SPP1. In the case of mass flow from SS, it is observed that the fine iron particles are lifted up by air flow forming a dust cloud above the avalanche (Fig. 4.14a). In SPP1, intermittent flow through the holes is recorded from the center to the rear end of the shoe, which reduces the effective area for the powder delivery. Also, low flow rate from the bottom layer results from air resistance to the flow of particles. The segregation due to the air flow is dominant for the iron powder used in this study that had a size range from 45-300 microns.

In the coloured salt experiments, apart from the commonly known nose flow and bulk flow in SS, a new flow named as standpipe flow using PP1 has been observed as shown in Fig. 4.1b. The standpipe flow exhibits a controlled flow and affects the flow patterns mainly by breaking the agglomerates of powder. In Fig. 4.12, a powder falling perpendicular to the direction of shoe motion is observed over a die-core near the centre of the die-cavity. This flow is more significant in SS than in SPP1. It is also observed that the flow from the holes of the perforated plate creates a stepped profile in the die (Fig. 4.13). The segregation of powder takes place separately during avalanche flow from each segment (from different holes) which results in different packing (mixed small and large particles arrangement) inside the die. However, in mass flow from SS, the segregation during the avalanche divides small (fine) particles in the bottom and large particles at the top. This results in uneven density distribution of powder inside the die.

The morphology of the particles for salt and iron is different, but still the segregation of salt layers from the shoe during its motion was found to be similar to the

segregation of iron powder layers in the shoe. It is evident that the rearrangement of particles and subsequent final packing of the powder in the die depends on the particle physical characteristics. As the salt particles are slightly bigger in size than iron particles (150-748 μm versus 45-300 μm), and size induced variation is also less; therefore, the salt layers in the die can be clearly distinguished, whereas, for iron powder, the layers are completely mixed due to immense friction and cohesiveness.

Lavoie et al. (2002) has indicated three stages of avalanche namely pre-avalanche stage, avalanche, and post-avalanche. He also explained that, at the time of an avalanche, two phenomena occur namely the distance travelled by the particles and the segregation of the surface. Both tend to affect the density distribution in the die-cavity. In this research, the post-avalanche angles were observed in the powder mass inside the shoe after the forward pass for different coloured powder experiments. These angles and the final packing of powder in the die explain the segregation of powder, and quantity of avalanched mass from different portions of the shoe during filling (Section 4.2-4.3).

Further, the displacement contours calculated using the in-situ ARAMIS optical system for different stages of the die filling process also demonstrate the segregation of powder during filling. The dynamic angle of repose (at the time of avalanche) during filling process using SS and SPP1 respectively are shown in Figs. 4.14a and b. Silva et al. (2000) identified different segregation mechanisms, out of which air flow, trajectory, angle of repose and percolation induced segregation are found to be dominant for this die-fill system. The air present inside the die during the filling process influences the small or fine particles distribution by entraining them. This is consistent with the fine

particle cloud above the slope of powder inside the die-cavity during the filling using standard shoe (Fig. 4.14a).

The next type of segregation noted is due to different types of flows; in nose flow the larger particles from the top free surface of the powder inside the shoe rapidly flow in the die-cavity, whereas the fine particles flows with low velocity due to strong frictional forces. Also, in bulk flow, the bottom particles flow later and slowly from the bottom due to the combined effect of friction between the base and the powder mass, and cohesion forces. These two flows occur successively. This mechanism was observed in the coloured powder experiments using SS (Section 4.2). Further, the segregation due to angle of repose plays a significant role in the distribution of the particles inside the die-cavity. It is evident that the powder with low angle of repose flows freely than the one with a higher angle of repose. However, in the kinematics of flow process, angle of repose of the powder changes, which is then referred as the dynamic angle of repose (Lavoie et al., 2002). The dynamic angle of repose obtained for SS and SPP1 filling shows a slight difference which indicate that the perforated plate decreases the avalanche angle and make the flow less intense (Fig. 4.14).

The net affect of the avalanche is that the smaller particles will sink to the bottom of the flowing stream and the larger particles will flow on the top (Makse et al., 1998). The interface of the flowing layer and the static pile can be viewed as a rough surface, where stopping probability of the smaller particles is higher than for larger particles (Fig. 4.14a). Thus, close to the filling point which is the right-side of the die in Fig. 4.14, the smaller particles settle at the foot of the avalanche and as more particles are added from

the flowing stream, the bottom particles spilt in two directions and slightly adjust along the x-axis. It is evident that the particles rolling down the slope of higher angle travel greater distance than those rolling on a small angle slope. Thus, the displacement in horizontal and vertical direction is greater in the die-cavity filled using SS than using SPP1. By using SPP1, it is realized that the standpipe flow is desirable in order to get a controlled vertical flow, which minimizes the vertical segregation, and less fine powder dust above the slope is observed (Fig. 4.14a versus b). In this sense, the use of perforated plate has significantly changed the avalanche mechanism which ultimately influences the distribution of the powder.

Another important feature of the avalanche is that the turbulent flow created in the die-cavity due to the air flow lifts the fine particles up near the top of the die. When the die-cavity gets filled due to the compressive force applied from the powder mass above the die; fine particles percolates through the voids between the large particles and, settle near the bottom. Therefore, bottom region is found to be with higher density than the top region (Section 4.7).

5.2. Effect of shoe velocity on flow behavior of powder

The experiments described in Chapter 4 explain the influence of shoe speed and use of perforated plate on the details of die filling process, and the way in which powder packs within the die. The shoe velocity affects the flow of powder mainly by changing the air flow inside the die, particle interlocking inside the shoe, and altering the intensity of flow. Wu et al. proposed that, for a simple die filling with a moving shoe, nose flow and bulk flow are observed to dominate the die filling at low and high shoe velocities

respectively. The results obtained by Wu were with the shoe velocities of 200 mm/s and 400 mm/s, which are similar to the velocities utilized in this research. However, the results analyzed from the coloured die filling experiments clearly demonstrate that, at a shoe velocity of 170 mm/s, the particles in the top layer flow at a slower rate in the die-cavity, and the bottom layer particles also get sufficient time to detach from the bulk; as the shoe moves slowly over the die-cavity. As a result, nose and bulk flow equally participate in the filling process (Fig. 4.2). In contrast, at a shoe velocity of 385 mm/s, the top surface particles are at a higher velocity than the bottom, and the bottom layer particles have limited time to separate from the cohesive mass of the powder; thus, nose flow dominate in the filling process (Fig. 4.3). This confirms that along with shoe velocity, particle morphology, physical properties of the powders, and the die geometry affects the flow mechanism. Wu and Cocks indicated that a shoe velocity at which nose flow dominates faster evacuation of air is achieved. In this study, at higher shoe velocity air evacuates quickly in the case of SS.

The avalanche phenomenon is utilized to understand the powder flow behavior during gravity filling at different shoe speeds. Particle morphology, forces of friction between the particles and the particles and the base, electrostatic forces, particle surface area, cohesion forces, are the various factors that act against gravity when the avalanche is about to occur. Thus, the way these parameters get influenced by the shoe speed affect the avalanche of powder, thereby changing the dynamic behavior of the powder. From Section 4.2, it is clear that the shoe velocity strongly affects the avalanche period in the powder flow as well as the post-avalanche slope.

Another fascinating observation is that in the case of SPP1, the shoe velocity does not seem to affect the particle arrangement inside the shoe; thus the sequence of flow and segregation of powder varies from the powder flow obtained using standard shoe. The SPP1 results show that the post-avalanche angle (powder profile in the shoe) in the shoe with tri-layer powder bed is relatively small near the top of the powder mass (Fig. 4.4). Also, the post-avalanche angle obtained for tri-column coloured powder experiments using PP1 slightly differ for the two shoe velocities utilized in the present work (Fig. 4.7). However, the angle at a shoe velocity of 385 mm/s changes for TCCS and TLCS powder bed using SPP1. The reason for the change is the different arrangement of powder bed which segregates different sizes of particles under gravity. Thus, during the shoe motion the powder flow pattern changes which ultimately change the avalanche behavior. The main reason for small change in the powder profile as compared to the big change in the powder profile of SS is due to the restrained motion of particles between the bottom of the perforated plate and the top of the die-cavity.

5.3. Effect of shoe velocity on average filling rate

During this research, the potential significance of the critical shoe velocity was explored for the ring-shaped die using ATOMET 1001 iron powder. The average filling rate of iron powder increases as the shoe velocity increases, for the SS case (Table 4.1). However, for SPP1 filling, the average filling rate increases as the shoe speed increases to the maximum speed of 170 mm/s, thereafter the filling rate decreases with increasing shoe velocity. Therefore, critical shoe velocities determined for the die filling using SS and SPP1 are 385 mm/s and 170 mm/s respectively (Table 4.1, Section 4.4). This is

because the powder flow from SPP1 occurs mainly from the bottom layer, where the flow rate from the rear perforated plate holes decreases due to air resistance and increase cohesion in the shoe. Thus, at higher shoe velocity rear portion of the shoe supplies small amount of powder this leads to incomplete filling. The present results for the filling rate using iron powder are consistent with the work of Wu et al., (2003a).

When the shoe translates at a lower velocity, mainly the front stream of powder is affected, and the filling thereby prolongs giving a low filling rate. As the shoe velocity increases, the particles from the front flow rapidly over the die-cavity, thereby giving a higher filling rate. However, the increase in the shoe velocity can enhance the interlocking of the particles, which is caused by the lateral compressive stresses generated by the inertia effects (Wu et al., 2003a). In SS filling, it is clear that as the shoe velocity increases, the rate of increase in the filling rate reduces. In SPP1 filling, it is found that the filling rate at 120 mm/s in SPP1 filling is higher than SS filling, whereas at 170 mm/s average filling rate is almost same. The reason for higher filling rate in SPP1 at low velocity is that the powder flows vertically with less turbulence. As a result, mass flow rate increases. However, the decrease in filling rate with the further increase in the shoe velocity for SPP1 filling is because of the interaction of air flow with the powder inside the holes in the rear side of the shoe, and strong interlocking between the particles in the back at high shoe velocity (Wu et al., 2003a). Above a shoe speed 240 mm/s, the trailing side (right-side) of the die remains partially filled. While in SS filling, large gap is created in the front of the shoe, when the shoe is moving at high velocity of 385 mm/s. As a result air evacuates efficiently from a standard shoe. Also, particles flow rapidly in

the die at high shoe velocity. Thus, critical velocity is higher for SS filling process. The average filling rate from the standard shoe increases with the addition of hopper, whereas minimal change in the filling rate is observed with hopper for SPP1 filling technique. The purpose of placing a hopper in front of the shoe is to continuously supply powder during filling to maintain the head pressure uniform in the shoe. A large gap in the front portion forms in SS during filling, whereas in SPP1 powder level inside the shoe does not change significantly. Thus, with the addition of hopper does not affect the quantity of mass flowing into the die in SPP1. In the coloured salt study, it is found that in SS with a hopper nose flow dominates and top two layers flow in with higher intensity, whereas, in SPP1, the pressure from the hopper powder mass is utilized in breaking the cohesion of the bottom layer particles. Therefore, no significant change in the filling rate is observed.

5.4. Effect of perforated plate on density distribution

A promising approach of introducing a perforated plate at the bottom of the shoe to modify the density distribution in the die filling condition was first proposed by Kim. In this research, further exploration of the perforated plate concept is performed to verify the uniformity of powder distribution during the die filling stage. A new design of perforated plate with circular holes of 0.16 inch diameter as shown in Fig. 3.5 was proposed. The usefulness of the perforated plates has been justified through various experiments conducted on the laboratory die filling set-up. Two designs of perforated plates were tested in this research. The experiments described in the Section 4.7 demonstrate the utility of PP1 for minimizing the porosity distribution.

A unique method of surface porosity measurement, using image analysis software, is suggested in this study. The images were recorded after the entire die filling cycle at six different locations on the die-cavity surface (transparent die-wall) as shown in Fig. 4.25. The results clearly demonstrate the positive effect of perforated plate addition to the bottom of the shoe in terms of the powder distribution and flow control. In Section 4.7, the top and bottom region porosity distribution in all the three regions (as per Fig. 4.25) for different filling techniques (from SS and SPP1) shows that the porosity distribution is highly uniform in the case of SPP1 filling.

By using PP1 (with straight holes), remarkably small difference of 0.6% is noted in the average porosity of all the locations. Thus, even distribution of metal powder is confirmed. A more controlled and less intense flow from the perforated plate appears to minimize the vertical segregation of powder during filling, which makes the powder distribution more uniform. The displacement contour results for powder flowing through a perforated plate in X and Y-direction demonstrates that the movement of particles along X or Y-axis is relatively small compared to the particle movement in the case of filling with SS (Fig. 4.15 – Fig. 4.22).

Another benefit of adding a perforated plate is that the powder mass in the holes of perforated plate holds equal amount of powder; thus, the packing pressure is uniform on the leading and trailing side of the die-cavity. However, from the gamma ray densitometry results regions (i.e., L2, R2, L3, and R3) of the ring-shaped part which are perpendicular to the direction of the shoe motion as shown in Fig. 4.28 show slightly nonuniform distribution with higher porosity. This means the powder distribution in the

regions perpendicular to the shoe motion is not significantly improved with the use of PP1.

The main drawback observed during the filling with PP1 is that the critical shoe velocity is lower than the standard shoe filling, which reduces the filling rate at higher shoe velocities. This problem can be solved by increasing the perforation diameter or changing array of the holes according to flow characteristics without affecting the controlled and uniform behavior of the flow.

Die filling with PP2 having slant holes at an angle of 15^{o} from the vertical axis showed only a minor variations in the powder flow, and the initial density distribution of powder in the die-cavity. More careful study is needed to determine the effect of hole-orientation on powder flow. It is realized that the orientation of holes in the perforated plate were made in the backward direction (i.e., towards the trailing side of the die), which was opposite, to the direction of powder flow. The free flow of powder became difficult as the powder stream had to turn its path of flow to enter into the hole. Thus, inconsistent flow was observed (Fig. 4.30). From the surface porosity distribution data for SS and SPP2 filling, the top and bottom region porosity varied significantly in SPP2. The most noticeable feature in SS filling is that the average porosity at T3 is 19% higher than B3; whereas for SPP2, T3 location has 30% higher porosity than B3.

Thus, it is understood that for getting a consistent flow, the orientation of slant holes should be changed and made in the same direction to that of powder flow as shown in Fig. 5.1.

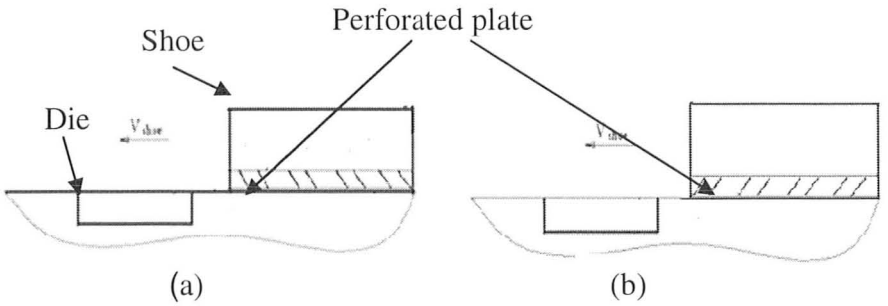

Figure 5.1. Hole orientation in a perforated plate, (a) Current pattern and (b) suggested pattern.

5.5. Feasibility of optical imaging system for die filling study

In-situ high-speed, high-resolution optical system ARAMIS based on Digital Image Correlation method is employed to track the particle displacements during die filling, and to understand the typical flow characteristics of the powder from a standard shoe and shoe with PP1. From the recorded images, it is possible to compare the displacement of particles at a specific location with the displacement of adjacent particles. In this study, the displacement traces of the particles in different stages of the filling process are plotted from the recorded images (Section 4.6). High-speed camera images have been analyzed by many researchers for an understanding of powder flow behavior and final packing of particles in the die. However, displacement tracking with the help of ARAMIS system in this study has been tried for the first time, in order to assess the segregation of the particles inside the die under various conditions.

It is noted that the top region particles rearranges differently than the bottom region particles in SS filling. A detailed assessment of the powder movement during die filling illustrated that the top particles displaces more than the bottom particles. Extra

powder is added to the die during the retraction stroke due to which particles in the top region of the die-cavity rearrange themselves along the x-axis. Also, due to the packing pressure from the powder mass inside the shoe, particles inside the die shift in the downward direction (along Y-axis).

During the forward stroke with SS, the nose flow of powder in the die pushes the powder entering later inside the die towards the right-side of the die (trailing side) along x-axis. Also, the turbulent flow of powder creates a fine dust cloud which segregates fine and coarse particles from the powder stream in the die. Therefore, both horizontal and vertical segregations are significant in SS. In the case of SPP1 filling, however, only horizontal segregation is found to be prominent; therefore, top and bottom porosity difference is not observed. In the intermediate stages of filling the bottom portion and the top right corner particles show uniform displacement along the vertical Y-axis, due to uniform packing pressure applied by the shoe. This means, in SPP1 filling, vertical segregation is negligible.

Thus, experimental results from the ARAMIS system confirm the usefulness of SPP1 and give a better understanding the cause of nonuniform distribution of powder during the die filling process.

5.6. Validation of powder sintering technique

A novel approach for ex-situ density measurement is explored in this research, by binding the powder in the die-fill condition using a thermoplastic resin. The die was filled by a mixture of iron and resin powder and low temperature heating of the filled die was performed to get a resin-bonded part. Similar operation was performed on the die filled

by SPP1. The sectioning on the heated part was done from different locations as shown in Fig. 4.28. Total six cut-samples from each part were tested on Gamma ray densitometry.

The X-ray tomography and sintering of the powder bed in filled condition were the two techniques utilized by Bruch et al. in 2008, to measure the density distribution in a filled die. They lightly sintered the powder (Distaloy AE) in the die-fill condition at 900°C at a rate of 5°C/min in an electrically heated furnace. The major concern with previous sintering technique is that the voids in the powder reduce in size due to the grain boundary movement at high-sintering temperature. Thus, it is obvious that the particles move from their original position, which will give inaccurate results about the actual die-fill distribution. Taking these challenges into consideration a new approach of binding the particles is introduced, in which secondary resin particles of low-melting point are mixed with the powder material. In this case, the sintering is carried out at 190°C, so that the liquid resin coats the iron particles without displacing them from the original position. In addition, the heating is controlled so that liquid resin does not push the iron particles. Also, the care is taken while cutting the sample to ensure that there is minimum pullout of the particles.

The results presented in this research are taken from the left and right sides of the heated ring-shaped part. The density calculated on each section with the mass and volume details is compared with the density obtained from the gamma ray densitometry.

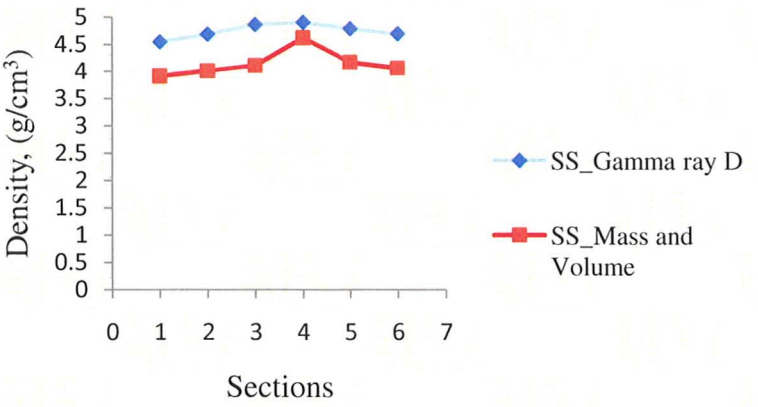

Figure 5.2. Comparison of die-fill density distribution by two techniques, for SS filling.

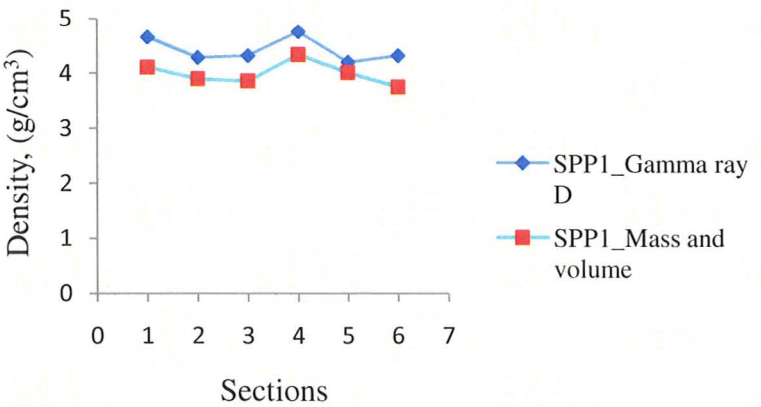

Figure 5.3. Comparison of die-fill density distribution by two techniques, for SPP1 filling.

In the above plots 1, 2, 3, 4, 5, and 6 along x-axis denote L1, L2, L3, R1, R2, and R3, respectively. Figs. 5.2 and 5.3 illustrates that the density values obtained by mass and volume method and gamma densitometry values differ slightly, but the trend is similar from both the techniques. Here in R3 section, higher density is observed. This is because of the two directional powder flows (Fig. 4.12 and Fig. 4.13) which give higher fill-density in the region (R3) near the centre of the die-cavity. However, Hjortsberg et al., (2002) had explained that for a ring-shaped die, the powder density is higher in the sections parallel to the direction of the shoe motion. The comparison plots above also confirm the results quoted by Hjortsberg.

From Table 4.3, it is noted that the void percentage is slightly higher in the SPP1 sample. The results obtained from the gamma ray densitometry also confirm that the average bulk porosity distribution in L1 and R1 sections (front sections) of the die filled sample, using SPP1, is even and higher than the other sections of the sample (Table 4.3). The comparison between the results obtained for the front region (i.e., L1 and R1) for SS and SPP1 from gamma ray densitometry technique are closer to those from the surface porosity measurement technique by image analyzer.

Georg, (2001) has explained the utility of gamma densitometry for testing powder based components. From this study, it is confirmed that gamma ray densitometry is very efficient way of measuring the voluminous density in a thick sample. Gamma ray spread in all directions, thus sample cutting can be eliminated, which will reduce the loss of particles from the surface, whereas in X-ray analysis the part has to be thin sectioned. In addition, X-ray tomography is costlier than gamma densitometry. The inconsistency in

the sintering technique can be solved by using a sintering furnace with nonoxidizing atmosphere, and most importantly by reducing the heating rate.

CHAPTER 6

CONCLUSIONS AND RECOMMENDATIONS

6.1. Conclusions

In this research several experiments were performed to understand the powder flow patterns and segregation from a shoe into a ring-shaped die-cavity. The density distribution in the die-fill condition results were also studied with the help of various techniques. Based on this study main conclusions are noted in this chapter.

With respect to the 1st objective of this research following conclusions can be drawn:

1. ARAMIS software with high speed camera is an efficient way of understanding and analyzing the powder flow behavior closely during the filling process. The perforated plate (PP1) gives controlled and less turbulent flow of the powder in the die-cavity whereas standard shoe filling gives a turbulent flow which causes the fine and coarse particles to strongly segregate in the die-cavity.
2. Flow rate of powder from the front portion of SPP1 is higher than the rear portion.
3. The displacement field data obtained using DIC method is effective in understanding the segregation of the particles in different regions of the die-cavity during the filling process with SS and SPP1.
4. The experimental studies with PP2 have not justified any benefits of changing the orientation of the holes in the perforated plate in backward direction (towards the trailing side of the die-cavity).

With respect to the 2nd and 3rd objectives following conclusions can be drawn:

1. The results on the powder flow pattern and segregation behavior at different shoe velocities from the coloured salt powder experiments confirm the utility of salt powder to mimic the iron powder flow macroscopically.
2. The effect of shoe velocity on the coloured salt powder flow has also clearly indicated that at low shoe velocity of 170 mm/s both nose flow and bulk flow takes part in filling whereas at high show velocity of 385 mm/s nose flow dominates (i.e., top surface particles flow at high velocity to fill the major portion of the die-cavity).
3. The effective area of discharge (i.e., the region in the shoe delivering the major amount of powder) can be evidently observed with the tri-column salt powder bed from SS and SPP1.
4. The avalanche characteristics of a powder alter with the use of perforate plate insert at the bottom of the shoe as well as by changing the arrangement of powder bed inside the shoe (i.e., tri-layer or tri-column).
5. In the filling process with SPP1, powder level inside the shoe changes slightly and maintains uniform packing weight on the leading and trailing side of the die-cavity.
6. From the filling rate experiments it is concluded that the critical velocity for SPP1 filling is lower than for SS filling that means higher filling rate cannot be obtained at the higher shoe velocity.
7. A hopper addition in a standard shoe increases the filling rate in the die-cavity.

With respect to the 4th and 5th objectives following conclusions can be drawn:

1. The pixel classifier program in the image analysis software is capable of determining the surface porosity in the powder mass for different locations on the die-cavity surface (transparent die-wall).
2. The results from the surface porosity measurement are in agreement with the displacement field data, which in turn validates the image analysis method for determining the surface porosity distribution in the die-cavity.

With respect to 6th and 7th objectives following conclusions can be drawn:

1. Resin bonding technique is an efficient way of binding the iron powder particles in the die-fill condition at low temperature of 195°C, and voluminous void data using gamma ray densitometry can be successfully obtained in different sections of the ring-shaped iron sample.
2. Gamma ray densitometry is a fast and accurate method of measuring the volume void fraction in the powder parts (i.e., loose or compacted parts) without affecting initial distribution of the powder.

6.2. Recommendations

There is a further need of investigating the perforated plate patterns for improving filling rate and density distribution in the entire die in filled condition. New designs of the perforated plate by changing the hole diameter, orientation of the holes or by changing the thickness of the plate should be tested to prove the effectiveness of the perforated plates over standard shoe filling.

There is a great potential in the displacement tracking of particles by using DIC method for understanding the particle interaction in the die-cavity during the filling process. Thus, the die walls should be made with a transparent material to observe and calculate the flow behavior of the particles in different locations of the die-cavity.

A small hopper use in this research has shown some benefits in improving the filling rate in the standard shoe. Therefore, a new hopper design with a suitable wall angle needs to be considered. Also, the study of the flow behaviour of the powder from a hopper is recommended to understand the effect of powder level in the hopper as well as the influence of the hopper location on the flow uniformity.

The resin bonding method followed by gamma ray densitometry technique needs to be explored further by comparing the density results obtained by resin-bonded sample with the density data obtained from the commonly used techniques such as X-ray tomography and pressure sensors method.

REFERENCES

C. Y. Wu and A.C.F Cocks and Oliver T. Gillia, "Die filling and powder transfer", International Journal of Powder Metallurgy, (2003a), Vol.39, No.4.

C. Y. Wu, A.C.F Cocks, O. T. Gillia, and D. A.Thompson, "Experimental and numerical investigations of powder transfer", Powder Technology, (2003b), Vol. 138, pp. 216-228.

C. Y. Wu, L. Dihoru, A. C. F. Cocks, " The flow of powder into simple and stepped dies", Powder Technology, (2003c), Vol. 134, pp.24-39.

C. Y. Wu and A.C.F. Cocks, "Flow behavior of powders during die filling", Powder Metallurgy, (2004), Vol. 47, No. 2, pp. 127-136.

C. Demetry, F. S.Souto, B. C. Ryden, and J.M. Roy, "Tactile sensing of density uniformity in powder beds after die filling", Powder Technology, (1998), pp. 119- 124.

D. Korachkin, D. T.Gethin, R. W. Lewis, J. H. Tweed, "Effect of die filling on powder compaction", Inter. J. of Powder Metallurgy,(2008), Vol. 44, 1.

De Silva, S., Dyroy, A., Enstad, G.G., "Segregation mechanisms and their quantification using segregation testers", IUTAM Symposium on Segregation in Granular Flows, (2000), Kluwer Academic Publishers, Boston, p.p. 11-29.

Dhanoa P. S. and Puri V. M., "Deposition of particulate materials confined spaces—New tester development and experimental results", Kona 16, (1998), pp. 152-159.

E. Hjortsberg and B. S. Bergquist, "Filling induced density variation in metal powder", Powder Metallurgy, (2002), Vol. 45, pp.146-153.

E.Verhulp, B.van Rietbergen*, R.Huiskes, "A three-dimensional digital image correlation technique for strain measurements in microstructures", Journal of Biomechanics, Vol.37, 1313–1320, 2004

Private communication from E. Emery: Flow properties of suitable pharmaceutical powders. Department of Chemical Engineering, University of Saskatchewan, September, 2008.

F. Motazedian , A.C.F Cocks, and I.C. Sinka, "The influence of airflow on gravity and suction filling", Department of Engineering, University of Leicester, (2007).

F. Lavoie, L. Cartilier, and R. Thibert, "New methods of characterizing avalanche behavior to determine powder flow", Pharmaceutical Research, 2002, Vol. 19, p. 6.

Georg .S, "Applying gamma ray densitometry in a PM production plant", Nuclear Engineering and Technology, 2001, Vol. 56, pp. 28-31.

G. M. Brasel, "Method of forming shaped components from mixtures of thermosetting binders and powders having a desired chemistry", US Patent no. : 5095387, 22nd October, 1991.

H.A. Makse and H.J Herrmann, "Microscopic model for microscopic granular stratification and segregation", Europhys. Lett., 1998, 43 (1), pp. 1-6.

H. A. Bruck, S. R. McNeill, M. A. Sutton and W. H. Peters, "Digital image correlation using Newton-Raphson method of partial differential correction ", Experimental Mechanics, Vol. 29, No. 3, 261-267, 1989.

James K. Prescott, Roger. A.B., "On powder flowability", Pharamceutical Technology, 2002.

J.P. Koeppe, M. Enz and J. Kakalios, "Phase diagram for avalanche stratification of granular media", Department of Astronomy, University of Minnesota, 1995.

M. Kim, "Improved density distribution in powder metallurgy parts with filtering method", Advanced Materials Research Vols. 26-28, 2007, pp. 445-448.

Sawayama, T., Seki, Y, "The effect of filling conditions on die filling", Advances in Powder Metallurgy & Particulate Materials, 2004, Vol. 1, pp. 61-72.

Schneider, L.C.R., Sinka, I.C. and Cocks, A.C.F, "Characterization of the flow behavior of pharmaceutical powders using a model die-shoe filling system", Powder Technology, 2007, Vol. 173, pp. 59-71.

S.F. Burch, A.C. F Cocks, J.M. Prado, and J.H. Tweed, "Die fill and powder transfer", Department of Engineering, University of Oxford, 2008.

S. C. Johnson, G. Angelo, M. Delucia, A. Herzing, "Powder handling and die filling: Introduction of rotary powder feeder method", Pennsylvania State University, 2002.

T. F. Zahrah and R. Rowland, "Fluidized Fill Shoe for Uniform Die Filling", P/M Science and Technology Briefs, 1999, Vol. 1, No. 3.

I.C Sinka, L.C. R. Schneider, A.C.F. Cocks," Measurement of the flow properties of powder with special reference to die fill", Inter. J. of Pharmaceutics 280, 2004, pp. 27-38.

I.C. Sinka , A.C.F. Cocks, " Evaluating flow behaviour of powders for die fill performance", Powder Metallurgy, Volume 52, Number 1, March 2009, pp. 8-11(4)

L.R. Lawrence and J.K Beddow, "Powder segregation during die filling", Powder Technology 2, (1968), pp. 125-130.

Private communication by Guo Yu: "A coupled DEM/CFD analysis for die filling process", Department of Chemical Engineering, University of Birmingham, 2010.

Parker J. R, "Gray level thresholding in badly illuminated images", IEEE transactions on pattern analysis and machine intelligence, (1991), Vol.13.

Reg Freeman and Xiao wei Fu, "Understanding die filling behaviour and its importance on final components", Powder Metallurgy, (2008), Vol. 51, pp. 196-201.

V.I. Faikin, V.P. Levin, Yu. N. Gribenyuk, "Influence of the rate of die filling on the density of the powder", Powder Metallurgy and Metal Ceramics,(1976), Vol. 15, pp.590-592.

X. Xie, V. M. Puri, "Uniformity of Powder Die Filling Using a Feed Shoe", A Review Particulate Science and Technology, Volume 24, Issue 4 December 2006, pp. 411- 426.

X. Xie, "Uniformity of simultaneous deposition of powder in multiple dies: measurement and modeling", Pennsylvania State University, (2006).